of *fecA1* and *fecA2* was PCR-amplified with specific biotinylated primers (*fecA1* promoter, forward 5′-Bio-GAAGCTTCCACCCTTTC-CAAATTATG and reverse 5′-CTTGATAGCTTTTTATGCGACTCAAATT; *fecA2* promoter, forward 5′-Bio-CATTCATTGTGATAACCTTTCTC and reverse 5′-AATAAATAACGCATTCTAAAACTAACAT). Biotinylated PCR products of the *fecA1* or *fecA2* promoter were immobilized onto Sensor Chip SA (GE Healthcare, Piscataway, NJ, USA). At least five concentrations of each purified Fur protein were applied to the *fecA1* or *fecA2* promoter-immobilized Sensor Chip SA in HBS-EP running buffer (10 mM Hepes, pH 7.4, 150 mM NaCl, 3 mM ethylenediaminetetraacetic acid, 0.005% surfactant P20) at a flow rate of 10 μl/min. The response value of the reference cell (flow cell 3, blank) was subtracted from the response values for each flow cell 4 (*fecA1* promoter-immobilized or *fecA2* promoter-immobilized) to correct for nonspecific binding. The measured values were expressed in resonance units proportional to the concentration of each Fur protein. The data were analyzed and the dissociation constant (K_d) values were calculated using BIAevaluation software (Biacore).

Measurement of SOD activity

The bacteria normalized to an OD_{600} of 1.0 were incubated under normal cultivation conditions or iron-restricted conditions (normal cultivation conditions with 20 μM deferoxamine mesylate) for 5 h. After sonication (1.5 min at 25% power) of the bacteria, the bacterial lysates were centrifuged, and then the SOD activity was measured using a SOD assay kit (Dojindo, Kumamoto, Japan) in accordance with the manufacturer's guidelines.

DNA sequencing of H. pylori sodB

The complete *sodB* gene was PCR-amplified with specific primers (forward 5′-ATTAACTTTTAAAAAATTTAAAAAGAATTTG and reverse 5′-TTAAGCTTTTTTATGCACC) using Ex Taq DNA polymerase (TaKaRa). The specific PCR products were direct-sequenced using the BigDye terminator version 1.1 cycle sequencing kit (Applied Biosystems, Foster City, CA, USA) and the deduced amino acid sequences were aligned using GENETYX version 5.1.

Disk assays for H_2O_2 susceptibility

The bacteria, normalized to an OD_{600} of 0.1, were plated for confluent growth on *Brucella* agar with or without 20 μM deferoxamine mesylate. Sterile 5-mm disks saturated with 10 μl of 5 M H_2O_2 were placed onto the plates. After 3 days, the zone of inhibition around the disks was measured.

Measurement of the MICs of Mtz

The bacteria, normalized to an OD_{600} of 0.1, were inoculated onto an agar plate containing Mtz in serial twofold dilutions (0.5–128 μg/ml) with or without 20 μM deferoxamine mesylate. After 3 days, the minimum inhibitory concentration (MIC) values were determined [22].

Measurement of the intracellular iron (Fe^{2+} and Fe^{3+}) concentration

The bacteria, normalized to an OD_{600} of 1.0, were incubated under normal cultivation conditions and iron-restricted conditions (normal cultivation conditions with 20 μM deferoxamine mesylate) for 5 h. After sonication (1.5 min at 25% power) of the bacteria, the bacterial lysates were centrifuged, and then the intracellular iron (Fe^{2+} and Fe^{3+}) concentration was measured using a Metalloassay Kit Fe (AKJ Global Technology Co., Chiba, Japan) in accordance with the manufacturer's guidelines. The data for the intracellular iron (Fe^{2+} and Fe^{3+}) concentration were corrected for total cellular protein.

Mongolian gerbil colonization studies

All experiments and procedures were carried out by the Keio University Animal Research Committee (08080-10). Six-week-old male specific-pathogen-free Mongolian gerbils (MON/Jms/Gbs Slc) ($n=42$) were purchased from Japan SLC. Seven-week-old animals were inoculated with one of the *fecA1* mutant *H. pylori* strains (ATCC700392, ATCC700392 *fecA1*-deletion mutant, KS0048, KS0048 *fecA1*-deletion mutant, KS0145, and KS0145 *fecA1*-deletion mutant); 0.6 ml of each bacterial suspension at a concentration of 10^9CFU/ml was administered using an orogastric catheter. Twelve weeks after the inoculation, the animals were sacrificed after 12 h of food deprivation and their stomachs were excised. One half of the tissues were weighed and homogenized in sterile saline, and the number of viable colony-forming units was determined by plating portions on Nissui *Helicobacter* agar (Nissui, Tokyo, Japan).

Statistical analysis

All values were expressed as means ± SD. The statistical significance of differences between the two groups was evaluated using the Student *t* test. The analysis was performed using the JSTAT statistical software (Version 8.2). Statistical significance was accepted at $P<0.05$, unless otherwise indicated.

Results

Enhancement of SodB activity and derepression of fecA1 mRNA expression in Mtz-resistant strains carrying mutant Fur

The SodB activity was significantly higher in the KS0048 and KS0145 strains compared with that in the ATCC700392 and KS0189 strains (Mtz-susceptible strains with wild-type Fur) under normal cultivation conditions (Fig. 2). Subsequently, in order to assess if amino acid mutation of SodB would contribute in the enhancement of its enzymatic activity, we aligned the predicted amino acid sequences of SodB for ATCC700392, KS0189, KS0048, and KS0145. No distinct amino acid mutation of the SodB protein was observed in the KS0048 and KS0145 strains (Supplementary Fig. 1). Based on these results, it is conceivable that KS0048 and KS0145 have an altered Fe^{2+} supply system for the SodB protein that enhances its enzymatic activity. Therefore, we next examined the iron (Fe^{2+} and Fe^{3+})-transport mechanisms of KS0048 and KS0145 in relation to the SodB activity. Initially, the mRNA expression of the *fecA* genes (*fecA1* and *fecA2*)

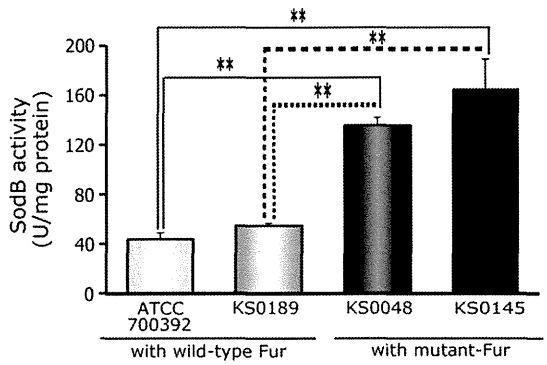

Fig. 2. Enhancement of SodB activity in the Mtz-resistant strains with mutant Fur under normal cultivation conditions. Under normal cultivation conditions, the SodB activity in ATCC700392 and KS0189 (Mtz-susceptible strains with wild-type Fur) and KS0048 and KS0145 (Mtz-resistant strains with mutant Fur) was measured by the method described under Materials and methods. Results are means ± SD of three independent assays. **$P<0.01$, statistically significant difference compared with the SodB activity in ATCC700392 and KS0189.

Please cite this article as: Tsugawa, H.; et al., FecA1, a bacterial iron transporter, determines the survival of *Helicobacter pylori* in the stomach, *Free Radic. Biol. Med.* (2012), doi:10.1016/j.freeradbiomed.2011.12.011

regulated by Fur was evaluated to assess whether expression of the Fe^{3+}-dicitrate transporter contributed to the increase in the SodB activity. The *fecA1* mRNA expression in KS0048 and KS0145 was significantly derepressed compared with that in ATCC700392 and KS0189 under normal cultivation conditions (Fig. 3A). Interestingly, the *fecA2* mRNA expression was not derepressed under normal cultivation conditions (Fig. 3B). These results suggest that the enhanced SodB activities of KS0048 and KS0145 were related to the increase in the Fe^{3+}-dicitrate uptake mediated by the *fecA1* gene. Next, to assess the mechanisms of *fecA1* mRNA derepression in KS0048 and KS0145, we aligned the nucleic acid sequences of the Fur-binding consensus sequence (Fur-box: AACTAATAATGGTTATT) of the *fecA1* promoter [15] and then examined the binding affinity of the iron-bound wild-type Fur and iron-bound mutant Fur to the promoters of *fecA1* and *fecA2* by surface plasmon resonance assay (BIAcore2000). No distinct mutation in the *fecA1* promoter was observed in KS0048 and KS0145 (data not shown). The K_d value of the binding of iron-bound mutant Fur to the *fecA1* and *fecA2* promoters as control was measured in comparison with that of iron-bound wild-type Fur. The results of the BIAcore assay revealed a significant increase in the K_d value for binding of iron-bound mutant Fur to the *fecA1* promoter compared with that of iron-bound wild-type Fur to the *fecA1* promoter (Fig. 3C), indicating a significantly reduced affinity of iron-bound mutant Fur for the *fecA1* promoter; therefore, *fecA1* expression was derepressed to a greater extent in KS0048 and KS0145 than in ATCC700392 and KS0189. On the other hand, the K_d value of iron-bound mutant Fur binding to the *fecA2* promoter did not increase (Fig. 3D), indicating that the amino acid mutations in Fur did not influence binding affinity to the *fecA2* promoter.

H_2O_2 sensitivity and Mtz resistance in the Mtz-resistant strains with mutant Fur under iron-restricted conditions

Next, we expected that the enhanced SodB activity in KS0048 and KS0145 might be repressed by iron-restricted conditions, to increase the H_2O_2 sensitivity and decrease Mtz resistance. First of all, to characterize the H_2O_2 sensitivity under iron-restricted conditions, we used an inhibition zone assay to comparatively examine the sensitivity of the ATCC700392, KS0189, KS0048, KS0145, and SodB-overexpressing mutants (ATCC700392 pHel3::sodB). The H_2O_2 sensitivity of KS0048, KS0145, and ATCC700392 pHel3::sodB was significantly decreased compared with that of ATCC700392 under normal cultivation conditions (Table 1). Under iron-restricted conditions, on the other hand, whereas the H_2O_2 sensitivity of ATCC700392 pHel3::sodB increased to the same level as that of ATCC700392, that of KS0048 and KS0145 was significantly lower compared with that of ATCC700392 (Table 1). Similarly, although the Mtz resistance of ATCC700392 pHel3::sodB (MIC = 32 μg/ml) [6] decreased to the level of Mtz sensitivity (MIC < 8 μg/ml) under iron-restricted conditions (MIC = 4 μg/ml), no decrease in the Mtz resistance of KS0048 and KS0145 was observed (Table 1). A possible reason for this finding is that the SodB activity was significantly higher in KS0048 and KS0145 compared with that in ATCC700392 and KS0189 under iron-

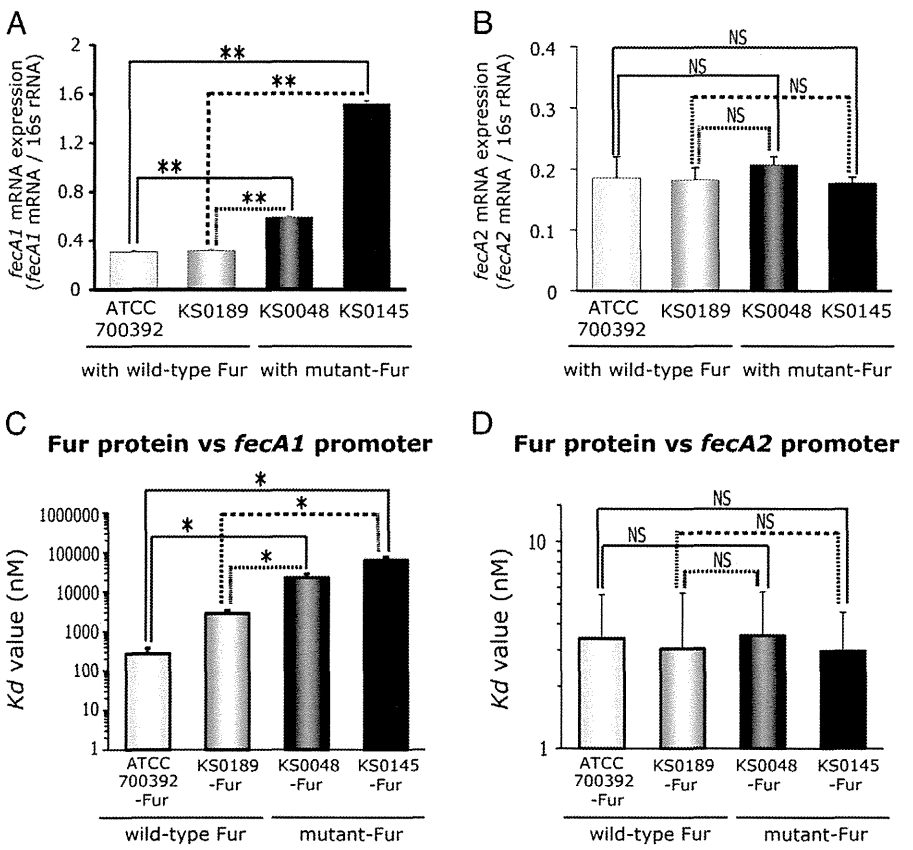

Fig. 3. Derepression of *fecA1* mRNA transcription by decreased affinity of mutant Fur for the *fecA1* promoter. (A) Under normal cultivation conditions, transcription of *fecA1* mRNA in ATCC700392 and KS0189, KS0048, and KS0145 was measured by quantitative RT-PCR. Results are means ± SD of three independent assays. $^{**}P<0.01$, statistically significant difference compared with the *fecA1* mRNA expression in ATCC700392 and KS0189. (B) Under normal cultivation conditions, transcription of *fecA2* mRNA in ATCC700392 and KS0189, KS0048, and KS0145 was measured by quantitative RT-PCR. Results are means ± SD of three independent assays. NS, not significant. (C) The K_d value for binding of each Fur protein to the *fecA1* promoter was calculated as a reference in the non-*fecA1* promoter-immobilized flow cells using BIAevaluation software. The white bar indicates the affinity of wild-type Fur for the *fecA1* promoter, and the black bar indicates the affinity of mutant Fur for the *fecA1* promoter. Results are means ± SD of three independent assays. $^{*}P<0.05$, statistically significant difference compared with ATCC700392-Fur and KS0189-Fur. (D) The K_d value for binding of each Fur protein to the *fecA2* promoter was calculated as a reference in the non-*fecA2* promoter-immobilized flow cells using BIAevaluation software. The white bar indicates the affinity of wild-type Fur for the *fecA2* promoter, and the black bar indicates the affinity of mutant Fur for the *fecA2* promoter. Results are means ± SD of three independent assays. NS, not significant.

Please cite this article as: Tsugawa, H.; et al., FecA1, a bacterial iron transporter, determines the survival of *Helicobacter pylori* in the stomach, *Free Radic. Biol. Med.* (2012), doi:10.1016/j.freeradbiomed.2011.12.011

Table 1
H_2O_2 and Mtz resistance of Mtz-resistant strains carrying mutant Fur under iron-restricted conditions.

Strain	Substitutions in Fur [6]	Iron-replete (normal cultivation) condition		Iron-restricted condition (20 μM deferoxamine mesylate)		
		Mean inhibition zone (mm)	*P* value	Mean inhibition zone (mm)	*P* value	MIC (μg/ml)
ATCC700392	Wild type	2.8±0.29		4.5±0.89		<0.5
KS0189	N118H	3.4±0.52	0.18	4.6±0.40	0.91	<0.5
KS0048	P114S, N118H	1.9±0.10	0.006**	2.2±0.25	0.013*	16
KS0145	C78Y, N118H	1.6±0.47	0.020**	2.1±0.12	0.042*	32
ATCC700392, pHel3::sodB	Wild type	1.6±0.45	0.019**	4.3±0.58	0.78	4
ATCC700392, pHel3 control	Wild type	3.0±0.45	0.69	4.5±0.30	1.0	2

Results are means ± SD of three independent assays.MIC, minimum inhibitory concentration (μg/mL).
*$P<0.05$ compared with ATCC700392.

restricted conditions (Fig. 4A). From this result, we expected that KS0048 and KS0145 might show enhanced iron (Fe^{2+} and Fe^{3+})-storage ability under normal cultivation conditions and then may make efficient reuse of the ferrous ion under iron-restricted conditions. Therefore, to examine the Fe^{2+}-storage ability of KS0048 and KS0145, we evaluated the mRNA expression of ferritin *pfr*, which is the major Fe^{2+}-storage protein regulated by Fur in *H. pylori* under normal cultivation conditions [23-25]. The expression levels of *pfr* mRNA in KS0048 and KS0145 were significantly increased compared with those in ATCC700392 and KS0189 under normal cultivation conditions (Fig. 4B). Actually, the levels of intracellular iron (Fe^{2+} and Fe^{3+}) in KS0048 and KS0145 were significantly higher than those in ATCC700392 and KS0189 under normal cultivation conditions (Fig. 4C). Additionally, under iron-restricted conditions, the *pfr* mRNA expression in the KS0048 and KS0145 strains was significantly derepressed compared with that in ATCC700392 and KS0189 (Fig. 4D), and the levels of intracellular iron in the KS0048 and KS0145 strains were also increased (Fig. 4E). These results suggested that KS0048 and KS0145 have an enhanced capability for ferrous ion storage by derepression of *pfr* under both normal cultivation and iron-restricted conditions.

Contribution of FecA1 to SodB activity, H_2O_2 sensitivity, and Mtz resistance

To characterize the contribution of FecA1 to the SodB activity, H_2O_2 sensitivity, and Mtz resistance of *H. pylori*, we constructed a *fecA1*-deletion mutant strain of each *H. pylori* strain (ATCC700392 *fecA1*-deletion mutant, KS0048 *fecA1*-deletion mutant, and KS0145 *fecA1*-deletion mutant). Deletion of the *fecA1* gene hardly influenced the bacterial growth in this study (data not shown). One reason for this may be that there was no decrease in the uptake of Fe ions (both $^{55}Fe^{2+}$ and $^{55}Fe^{3+}$) into the bacterial cells of the *fecA1*-deletion mutant strains [26]. The SodB activity of all *fecA1*-deletion mutant strains was significantly decreased (Fig. 5A). The SodB activity of ATCC700392 was the most significantly decreased with *fecA1* deletion, suggesting that Fe^{2+} is supplied to SodB through FecA1 in *H. pylori*, regardless of the presence/absence of amino acid mutations in Fur. Similarly, the H_2O_2 resistance of each *fecA1*-deletion mutant was significantly decreased by 30–60% (Fig. 5B). In addition, the MICs of Mtz for KS0048 and KS0145 decreased dramatically from 32 to 4 and from 128 to 32 μg/ml, respectively. Especially, the Mtz resistance of KS0048 was completely reversed by *fecA1* deletion (MIC<8 μg/ml). To assess whether derepression of *fecA1* mRNA expression was dependent on mutant Fur, we measured the MIC of Mtz in a *fecA1*-deletion mutant of ATCC43504. Development of Mtz resistance in ATCC43504 was caused by the deletion of the *rdxA* gene [18]. Alignment of the predicted amino acid sequences of ATCC43504-Fur showed that ATCC43504-Fur was the wild type. This sequence showed a 100% homology with KS0189-Fur (data not shown). The MIC of Mtz for ATCC43504 decreased slightly (from 128 to 64 μg/ml) after *fecA1* deletion. This finding demonstrated that development of Mtz resistance by FecA1 depended on the mutant Fur.

Colonization of Mongolian gerbils by the fecA1-deletion mutant

To assess the role of FecA1 in the host-colonization ability of *H. pylori*, we measured the colonization of the gastric mucosa by wild-type and *fecA1*-deletion mutant strains at 12 weeks after inoculation into Mongolian gerbils. The *fecA1*-deletion mutant of ATCC700392 tended to show reduced host colonization compared with the wild-type ATCC700392 ($P=0.050$; Fig. 6). The *fecA1*-deletion mutants KS0048 and KS0145 showed a significantly reduced capability for host colonization compared with the wild type of each strain ($P=0.014$ and $P=0.016$, respectively; Fig. 6). Our finding did not indicate whether the host-colonization abilities of KS0048 and KS0145 were significantly increased compared with that of the ATCC700392 (Fig. 6). This result suggested that derepression of *fecA1* by mutant Fur alone did not lead to enhanced host colonization.

Discussion

H. pylori encodes only one single iron (Fe^{2+})-cofactored SOD (SodB). Therefore, ferrous ion is indispensable for activation of SOD in *H. pylori* [8]. Our findings indicate that the enhanced Fe^{2+}-supply system associated with SodB activation in the KS0048 and KS0145 strains can be explained as follows: under iron-replete conditions, Fe^{3+}-dicitrate transport was enhanced by derepression of *fecA1* mRNA expression by iron-bound mutant Fur. Intracellular ferric ion (Fe^{3+}) was reduced to Fe^{2+} by Fe^{3+}-reductase (ribBA) [27], providing Fe^{2+} to SodB (Fig. 7). Under iron-restricted conditions, Fe^{2+} storage in KS0048 and KS0145 was enhanced through derepression of *pfr* mRNA expression by apo-mutant Fur, supplying Fe^{2+} to SodB (Fig. 7). In addition, our results demonstrated, for the first time, that FecA1 may play an indispensable role in the bacterial survival in the stomach and in the development of Mtz resistance of *H. pylori* through Fe^{2+} supply to SodB.

Because *H. pylori* is a highly genetically diverse organism, different strains may show great variations in phenotype. However, in this study, all *fecA1*-deletion mutant strains of *H. pylori* (ATCC700392, KS0048, and KS0145) showed reduced SodB activity and reduced gastric mucosal colonization ability. Therefore, it is thought that Fe^{3+}-dicitrate transport by FecA1 is associated with the activation of SodB, regardless of the genetic diversity of the strains.

The *fecA1* and *fecA2* genes, encoded in *H. pylori* as a Fe^{3+}-dicitrate transporter, are both regulated by Fur [10,11]. In this study, interestingly, in KS0048 and KS0145, only *fecA1* expression was derepressed by mutant Fur under normal cultivation conditions (Fig. 3A), whereas the expression of *fecA2* was repressed (Fig. 3B). The underlying reason was the high affinity of iron-bound wild-type Fur for the *fecA2* promoter compared with that for the *fecA1* promoter; the K_d value of iron-bound wild-type Fur binding to the *fecA2* promoter ($K_d=3.4$ nM) was low compared with that to the *fecA1* promoter ($K_d=273$ nM) (Figs. 3C and D). This result suggested that the expression of *fecA1*, but not of *fecA2*, was more influenced by amino acid mutations in Fur, and then only the expression of *fecA1* was derepressed by mutant Fur. Recently, Ernst et al. [5] reported that the K_d value for the *sodB* promoter of apo-wild-type Fur was also low ($K_d=270$ nM, from the data of [5]), similar to the K_d value for the *fecA1* promoter of iron-bound wild-type Fur. Because *H. pylori* is continuously exposed to superoxides generated by its own respiration and metabolism and the

Please cite this article as: Tsugawa, H.; et al., FecA1, a bacterial iron transporter, determines the survival of *Helicobacter pylori* in the stomach, *Free Radic. Biol. Med.* (2012), doi:10.1016/j.freeradbiomed.2011.12.011

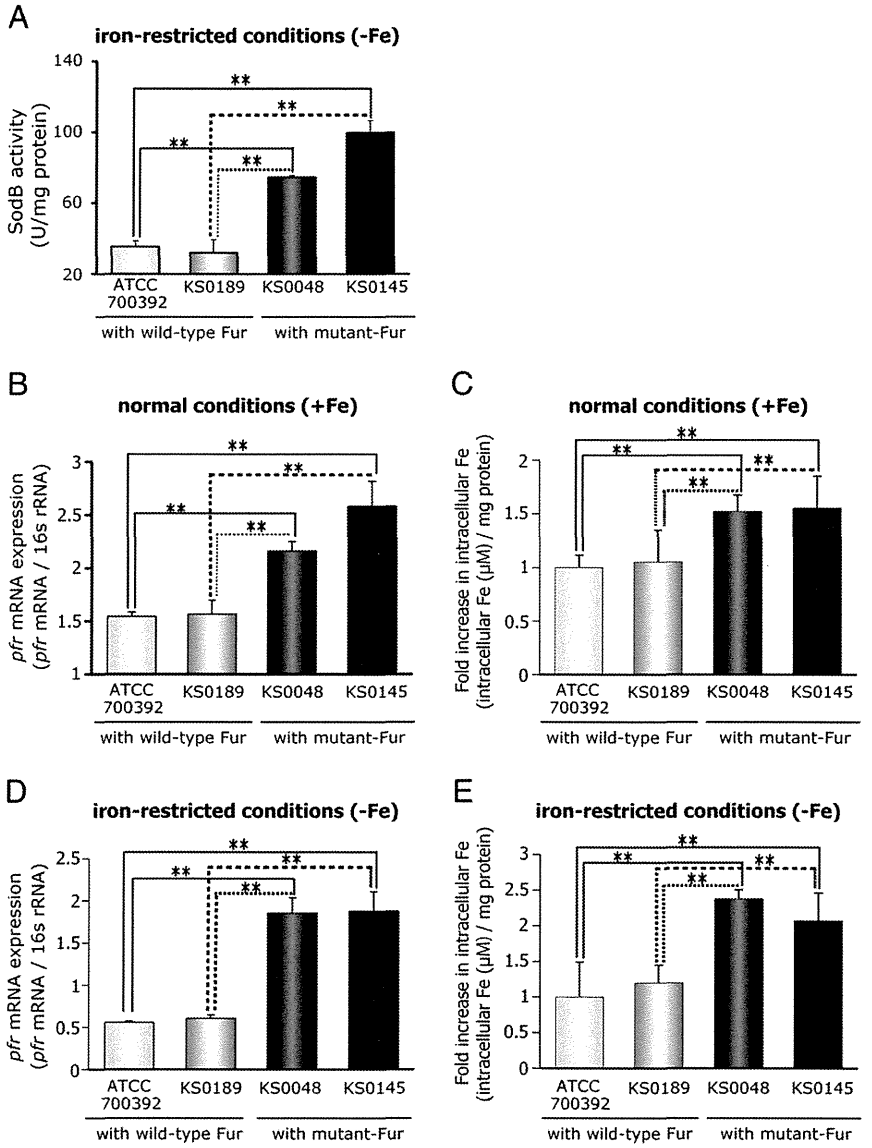

Fig. 4. SodB activity of the Mtz-resistant strains with mutant Fur under iron-restricted conditions was supported by the increase in the iron-storage ability. (A) Under iron-restricted conditions, the SodB activity in ATCC700392, KS0189, KS0048, and KS0145 was measured by the method described under Materials and methods. Results are means ± SD of three independent assays. $^{**}P<0.01$, statistically significant difference compared with the SodB activity in ATCC700392 and KS0189. (B) Under normal cultivation conditions, expression of *pfr* mRNA in ATCC700392, KS0189, KS0048, and KS0145 was measured by quantitative RT-PCR. Results are means ± SD of three independent assays. $^{**}P<0.01$, statistically significant difference compared with *pfr* mRNA expression in ATCC700392 and KS0189. (C) Under normal cultivation conditions, intracellular iron (Fe^{2+} and Fe^{3+}) concentration was measured by the method described under Materials and methods. The data for the intracellular iron concentration were corrected by total cellular protein. Results are means ± SD of three independent assays. $^{**}P<0.01$, statistically significant difference compared with the intracellular iron concentration in ATCC700392 and KS0189. (D) Under iron-restricted conditions, expression of *pfr* mRNA in ATCC700392, KS0189, KS0048, and KS0145 was measured by quantitative RT-PCR. Results are means ± SD of three independent assays. $^{**}P<0.01$, statistically significant difference compared with *pfr* mRNA expression in ATCC700392 and KS0189. (E) Under iron-restricted conditions, intracellular iron (Fe^{2+} and Fe^{3+}) concentration was measured by the method described under Materials and methods. Results are means ± SD of three independent assays. $^{**}P<0.01$, statistically significant difference compared with the intracellular iron concentration in ATCC700392 and KS0189.

host immune response, sustained expression of SodB activity is required for the dismutation of such superoxides [28,29]. Hence, it is thought that a low affinity of apo-Fur and iron-bound Fur for the *sodB* and *fecA1* promoters, respectively, is required for efficient and persistent activation of SodB.

In *H. pylori*, Fur regulates the gene expression of both iron-bound and apo-Fur [11]. *sodB* mRNA expression is repressed by apo-Fur; on the other hand, *fecA1* mRNA expression is repressed by iron-bound Fur [5,14,15]. In fact, despite the difference in the binding patterns of Fur to the *sodB* promoter and *fecA1* promoter, the mRNA expression of both *sodB* and *fecA1* was co-derepressed by mutant Fur (Fig. 3) [6], suggesting that the amino acid mutations (C78Y and P114S) in Fur alter its binding to promoter DNA, but not to Fe^{2+}. *H. pylori* Fur monomer contains two domains, the N-terminal DNA-binding domain and the C-terminal dimerization domain with metal-binding sites, and after dimerization, the Fur protein binds to the target promoter DNA [6,30]. We showed, using homology modeling, that the mutation C78Y was localized in the DNA-binding domain, whereas P114S was localized in the oligomerization domain [6]. Changes in the target-DNA binding of Fur by amino acid mutation have been categorized into the following two groups: (i) effects on the binding ability of Fe^{2+} and (ii) effects on dimerization [30]. Dian et al. identified the S2 functional domain, which was essential for dimerization in *H. pylori* Fur [31]. According to that report, replacement of Cys 78 with tyrosine is predicted to interfere with the formation of the S2 site [31].

Please cite this article as: Tsugawa, H.; et al., FecA1, a bacterial iron transporter, determines the survival of *Helicobacter pylori* in the stomach, *Free Radic. Biol. Med.* (2012), doi:10.1016/j.freeradbiomed.2011.12.011

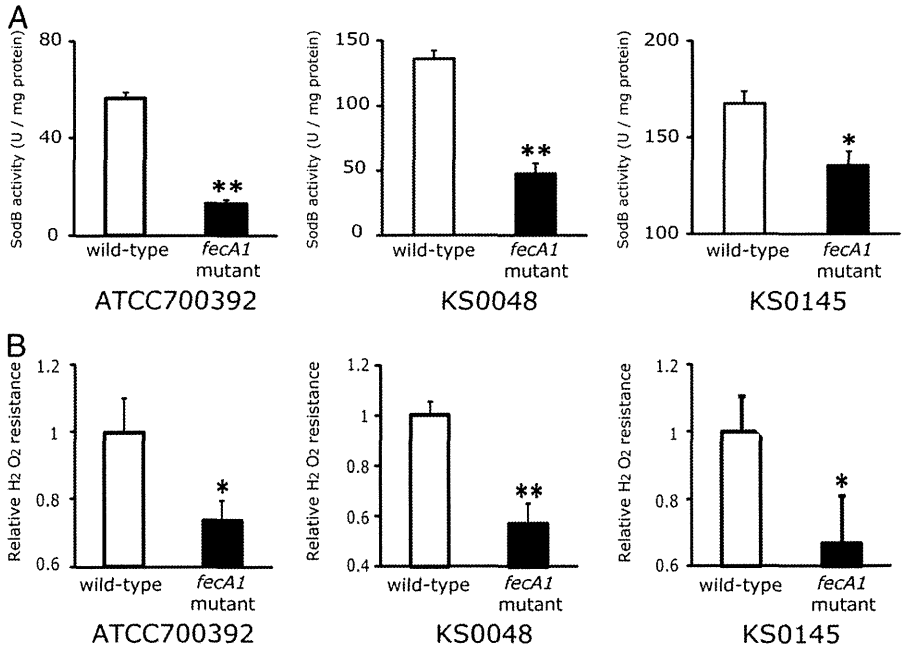

Fig. 5. Deletion of *fecA1* reduces SodB activity and H_2O_2 resistance. (A) The *fecA1*-deletion mutant was constructed as described under Materials and methods. The SodB activity in the wild-type and *fecA1*-deletion mutants for each strain was measured as described under Materials and methods. The results are expressed as means ± SD of three independent assays. $^*P<0.05$, $^{**}P<0.01$, statistically significant difference compared with the wild-type for each strain. (B) H_2O_2 resistance was measured by the inhibition zone assay described under Materials and methods. The results are means ± SD of three independent assays. $^*P<0.05$, $^{**}P<0.01$, statistically significant difference compared with the wild-type for each strain.

Our in vivo studies demonstrated that the colonization ability of *H. pylori* in Mongolian gerbils was greatly impaired by *fecA1* deletion, regardless of the presence of Fur mutation. From this result, it is thought that the SodB activation in *H. pylori* is supported by Fe^{2+} supply through FecA1 to combat the oxidative stress evoked by the host immune response. Because recently there has been a gradual increase in reports of multiple-drug-resistant *H. pylori*, the development of a novel bactericidal therapy, different from antibiotics, is required. FecA1 is one possible target for the development of a novel bactericidal therapy as well as possibly a preventive therapy against *H. pylori* infection.

In conclusion, Fe^{3+}-dicitrate transport by FecA1 is an essential process in the activation of SodB, which determines the gastric mucosal colonization ability of *H. pylori* in Mongolian gerbils and also the development of Mtz resistance.

Supplementary data associated with this article can be found in the online version at doi:10.1016/j.freeradbiomed.2011.12.011.

Acknowledgments

The authors are grateful to Misa Kanekawa for her technical assistance. This work was supported by a Grant-in-Aid for Young Scientists

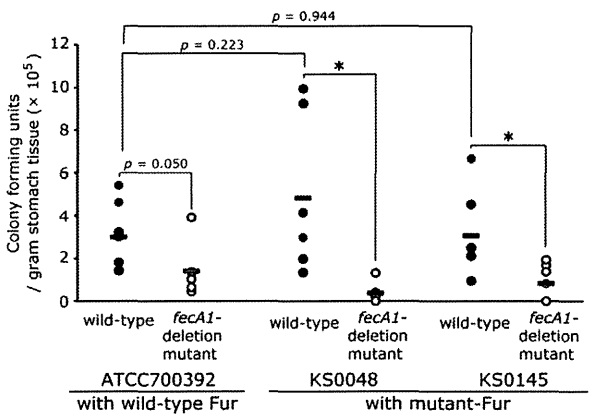

Fig. 6. Deletion of *fecA1* reduces the ability of *H. pylori* to colonize the stomach of Mongolian gerbils. Total colonization of the stomach was determined by sacrificing the animals at 12 weeks, and the results were expressed as the number of CFU/g of stomach tissue. Mongolian gerbils were infected with either a wild-type *H. pylori* strain (filled circle) or a *fecA1*-deletion mutant *H. pylori* strain (open circle). Each circle indicates the results for a single animal. The geometric means are indicated by bars. $^*P<0.05$, statistically significant difference compared with the wild type.

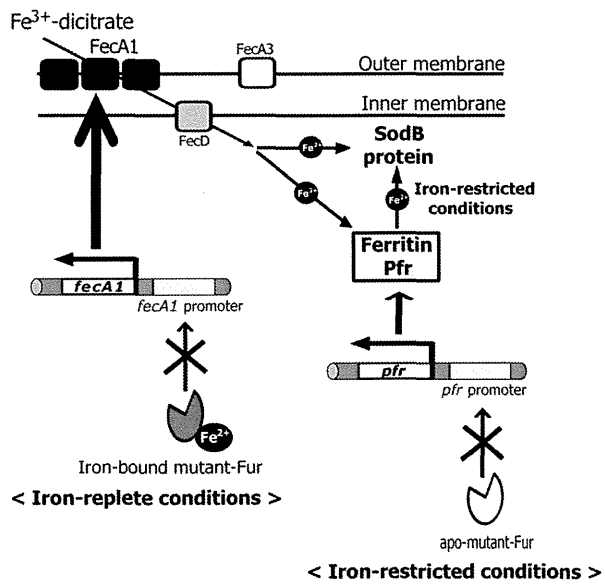

Fig. 7. Schematic representation of the ferrous ion (Fe^{2+})-supply system to the SodB protein in the Mtz-resistant strains with mutant Fur. Under iron-replete conditions, *fecA1* mRNA expression is derepressed by iron-bound mutant Fur, and then Fe^{2+} is supplied to the SodB protein. Under iron-restricted conditions, the capability of Fe^{2+} storage in the KS0048 and KS0145 strains is enhanced by derepression of *pfr* mRNA expression by apo-mutant Fur, and then Fe^{2+} is supplied to SodB from Pfr.

(B) (23790156, to H.T.) and a Grant-in-Aid for Scientific Research B (22300169 to H.S.) from the Japan Society for the Promotion of Science, a grant from the Adaptable and Seamless Technology Transfer Program through Target-Driven R&D (A-STEP) (AS231Z00132G to H.S.) of the Japan Science and Technology Agency, a grant from the Strategic Basis on Research Grounds for Nongovernmental Schools of the Ministry of Education, Culture, Sports, Science, and Technology (to H.S.), a grant from the Smoking Research Foundation (to H.S.), and the Keio Gijuku Academic Development Fund (to H.S.). This work was awarded the Prize for Best Investigator (ICAT award) at the Fifth Inflammation in Alimentary Tract Conference.

References

[1] Suzuki, H.; Hibi, T.; Marshall, B. J. *Helicobacter pylori*: present status and future prospects in Japan. *J. Gastroenterol.* **42:**1–15; 2007.
[2] Wang, G.; Alamuri, P.; Maier, R. J. The diverse antioxidant systems of *Helicobacter pylori*. *Mol. Microbiol.* **61:**847–860; 2006.
[3] Bereswill, S.; Neuner, O.; Strobel, S.; Kist, M. Identification and molecular analysis of superoxide dismutase isoforms in *Helicobacter pylori*. *FEMS Microbiol. Lett.* **183:** 241–245; 2000.
[4] Spiegelhalder, C.; Gerstenecker, B.; Kersten, A.; Schiltz, E.; Kist, M. Purification of *Helicobacter pylori* superoxide dismutase and cloning and sequencing of the gene. *Infect. Immun.* **61:**5315–5325; 1993.
[5] Ernst, F. D.; Homuth, G.; Stoof, J.; Mader, U.; Waidner, B.; Kuipers, E. J.; Kist, M.; Kusters, J. G.; Bereswill, S.; van Vliet, A. H. Iron-responsive regulation of the *Helicobacter pylori* iron-cofactored superoxide dismutase SodB is mediated by Fur. *J. Bacteriol.* **187:**3687–3692; 2005.
[6] Tsugawa, H.; Suzuki, H.; Satoh, K.; Hirata, K.; Matsuzaki, J.; Saito, Y.; Suematsu, M.; Hibi, T. Two amino acids mutation of ferric uptake regulator determines *Helicobacter pylori* resistance to metronidazole. *Antioxid. Redox Signal.* **14:**15–23; 2011.
[7] Seyler Jr., R. W.; Olson, J. W.; Maier, R. J. Superoxide dismutase-deficient mutants of *Helicobacter pylori* are hypersensitive to oxidative stress and defective in host colonization. *Infect. Immun.* **69:**4034–4040; 2001.
[8] Esposito, L.; Seydel, A.; Aiello, R.; Sorrentino, G.; Cendron, L.; Zanotti, G.; Zagari, A. The crystal structure of the superoxide dismutase from *Helicobacter pylori* reveals a structured C-terminal extension. *Biochim. Biophys. Acta* **1784:**1601–1606; 2008.
[9] Touati, D. Iron and oxidative stress in bacteria. *Arch. Biochem. Biophys.* **373:**1–6; 2000.
[10] van Vliet, A. H.; Stoof, J.; Vlasblom, R.; Wainwright, S. A.; Hughes, N. J.; Kelly, D. J.; Bereswill, S.; Bijlsma, J. J.; Hoogenboezem, T.; Vandenbroucke-Grauls, C. M.; Kist, M.; Kuipers, E. J.; Kusters, J. G. The role of the ferric uptake regulator (Fur) in regulation of *Helicobacter pylori* iron uptake. *Helicobacter* **7:**237–244; 2002.
[11] Ernst, F. D.; Bereswill, S.; Waidner, B.; Stoof, J.; Mader, U.; Kusters, J. G.; Kuipers, E. J.; Kist, M.; van Vliet, A. H.; Homuth, G. Transcriptional profiling of *Helicobacter pylori* Fur- and iron-regulated gene expression. *Microbiology* **151:**533–546; 2005.
[12] Ernst, F. D.; Stoof, J.; Horrevoets, W. M.; Kuipers, E. J.; Kusters, J. G.; van Vliet, A. H. NikR mediates nickel-responsive transcriptional repression of the *Helicobacter pylori* outer membrane proteins FecA3 (HP1400) and FrpB4 (HP1512). *Infect. Immun.* **74:**6821–6828; 2006.
[13] Danielli, A.; Romagnoli, S.; Roncarati, D.; Costantino, L.; Delany, I.; Scarlato, V. Growth phase and metal-dependent transcriptional regulation of the fecA genes in *Helicobacter pylori*. *J. Bacteriol.* **191:**3717–3725; 2009.
[14] Delany, I.; Pacheco, A. B.; Spohn, G.; Rappuoli, R.; Scarlato, V. Iron-dependent transcription of the frpB gene of *Helicobacter pylori* is controlled by the Fur repressor protein. *J. Bacteriol.* **183:**4932–4937; 2001.
[15] Merrell, D. S.; Thompson, L. J.; Kim, C. C.; Mitchell, H.; Tompkins, L. S.; Lee, A.; Falkow, S. Growth phase-dependent response of *Helicobacter pylori* to iron starvation. *Infect. Immun.* **71:**6510–6525; 2003.
[16] Allen, L. A. Phagocytosis and persistence of *Helicobacter pylori*. *Cell. Microbiol.* **9:** 817–828; 2007.
[17] Olczak, A. A.; Olson, J. W.; Maier, R. J. Oxidative-stress resistance mutants of *Helicobacter pylori*. *J. Bacteriol.* **184:**3186–3193; 2002.
[18] Debets-Ossenkopp, Y. J.; Pot, R. G.; van Westerloo, D. J.; Goodwin, A.; Vandenbroucke-Grauls, C. M.; Berg, D. E.; Hoffman, P. S.; Kusters, J. G. Insertion of mini-IS605 and deletion of adjacent sequences in the nitroreductase (rdxA) gene cause metronidazole resistance in *Helicobacter pylori* NCTC11637. *Antimicrob. Agents Chemother.* **43:** 2657–2662; 1999.
[19] Heuermann, D.; Haas, R. A stable shuttle vector system for efficient genetic complementation of *Helicobacter pylori* strains by transformation and conjugation. *Mol. Gen. Genet.* **257:**519–528; 1998.
[20] Tsugawa, H.; Ogawa, A.; Takehara, S.; Kimura, M.; Okawa, Y. Primary structure and function of a cytotoxic outer-membrane protein (ComP) of *Plesiomonas shigelloides*. *FEMS Microbiol. Lett.* **281:**10–16; 2008.
[21] Osaki, T.; Hanawa, T.; Manzoku, T.; Fukuda, M.; Kawakami, H.; Suzuki, H.; Yamaguchi, H.; Yan, X.; Taguchi, H.; Kurata, S.; Kamiya, S. Mutation of luxS affects motility and infectivity of *Helicobacter pylori* in gastric mucosa of a Mongolian gerbil model. *J. Med. Microbiol.* **55:**1477–1485; 2006.
[22] Nagayama, A.; Yamaguchi, K.; Watanabe, K.; Tanaka, M.; Kobayashi, I.; Nagasawa, Z. Final report from the Committee on Antimicrobial Susceptibility Testing, Japanese Society of Chemotherapy, on the agar dilution method (2007). *J. Infect. Chemother.* **14:**383–392; 2008.
[23] Bereswill, S.; Waidner, U.; Odenbreit, S.; Lichte, F.; Fassbinder, F.; Bode, G.; Kist, M. Structural, functional and mutational analysis of the pfr gene encoding a ferritin from *Helicobacter pylori*. *Microbiology* **144:**2505–2516; 1998.
[24] Doig, P.; Austin, J. W.; Trust, T. J. The *Helicobacter pylori* 19.6-kilodalton protein is an iron-containing protein resembling ferritin. *J. Bacteriol.* **175:**557–560; 1993.
[25] Frazier, B. A.; Pfeifer, J. D.; Russell, D. G.; Falk, P.; Olsen, A. N.; Hammar, M.; Westblom, T. U.; Normark, S. J. Paracrystalline inclusions of a novel ferritin containing nonheme iron, produced by the human gastric pathogen *Helicobacter pylori*: evidence for a third class of ferritins. *J. Bacteriol.* **175:**966–972; 1993.
[26] Velayudhan, J.; Hughes, N. J.; McColm, A. A.; Bagshaw, J.; Clayton, C. L.; Andrews, S. C.; Kelly, D. J. Iron acquisition and virulence in *Helicobacter pylori*: a major role for FeoB, a high-affinity ferrous iron transporter. *Mol. Microbiol.* **37:**274–286; 2000.
[27] Worst, D. J.; Gerrits, M. M.; Vandenbroucke-Grauls, C. M.; Kusters, J. G. *Helicobacter pylori* ribBA-mediated riboflavin production is involved in iron acquisition. *J. Bacteriol.* **180:**1473–1479; 1998.
[28] Demple, B. Regulation of bacterial oxidative stress genes. *Annu. Rev. Genet.* **25:** 315–337; 1991.
[29] Leclere, V.; Chotteau-Lelievre, A.; Gancel, F.; Imbert, M.; Blondeau, R. Occurrence of two superoxide dismutases in *Aeromonas hydrophila*: molecular cloning and differential expression of the sodA and sodB genes. *Microbiology* **147:** 3105–3111; 2001.
[30] Carpenter, B. M.; Gancz, H.; Benoit, S. L.; Evans, S.; Olsen, C. H.; Michel, S. L.; Maier, R. J.; Merrell, D. S. Mutagenesis of conserved amino acids of *Helicobacter pylori* fur reveals residues important for function. *J. Bacteriol.* **192:**5037–5052; 2011.
[31] Dian, C.; Vitale, S.; Leonard, G. A.; Bahlawane, C.; Fauquant, C.; Leduc, D.; Muller, C.; de Reuse, H.; Michaud-Soret, I.; Terradot, L. The structure of the *Helicobacter pylori* ferric uptake regulator Fur reveals three functional metal binding sites. *Mol. Microbiol.* **79:**1260–1275; 2011.

Please cite this article as: Tsugawa, H.; et al., FecA1, a bacterial iron transporter, determines the survival of *Helicobacter pylori* in the stomach, *Free Radic. Biol. Med.* (2012), doi:10.1016/j.freeradbiomed.2011.12.011

Biochemical and Biophysical Research Communications 420 (2012) 444–449

Contents lists available at SciVerse ScienceDirect

Biochemical and Biophysical Research Communications

journal homepage: www.elsevier.com/locate/ybbrc

Effects of β-(1,3–1,6)-D-glucan on irritable bowel syndrome-related colonic hypersensitivity

Teita Asano [a], Ken-ichiro Tanaka [b], Shintaro Suemasu [a], Tomoaki Ishihara [a], Kayoko Tahara [a], Toshio Suzuki [c], Hidekazu Suzuki [d], Shin Fukudo [e], Tohru Mizushima [a,b,*]

[a] Department of Analytical Chemistry, Faculty of Pharmacy, Keio University, Tokyo 105-8512, Japan
[b] Graduate School of Medical and Pharmaceutical Sciences, Kumamoto University, Kumamoto 862-0973, Japan
[c] Research and Development, Daiso Co., Ltd., Amagasaki 660-0842, Japan
[d] Division of Gastroenterology and Hepatology, Department of Internal Medicine, Keio University School of Medicine, Tokyo 160-8582, Japan
[e] Department of Behavioral Medicine, Tohoku University Graduate School of Medicine, Sendai 980-8575, Japan

ARTICLE INFO

Article history:
Received 29 February 2012
Available online 10 March 2012

Keywords:
Irritable bowel syndrome
Fecal pellet output
Visceral pain response
β-Glucan

ABSTRACT

Irritable bowel syndrome (IBS) is a gastrointestinal disorder characterized by chronic abdominal pain associated with altered bowel habits. Since the prevalence of IBS is very high and thus, involves elevated health-care costs, treatment of this condition by methods other than prescribed medicines could be beneficial. β-(1,3)-D-glucan with β-(1,6) branches (β-glucan) has been used as a nutritional supplement for many years. In this study, we examined the effect of β-glucan on fecal pellet output and visceral pain response in animal models of IBS. Oral administration of β-glucan suppressed the restraint stress- or drug-induced fecal pellet output. β-Glucan also suppressed the visceral pain response to colorectal distension. These results suggest that β-glucan could be beneficial for the treatment and prevention of IBS.

1. Introduction

IBS is a functional gastrointestinal disorder characterized by chronic and recurrent abdominal pain and discomfort (colonic hypersensitivity) that are associated with altered bowel habits but not with any detectable structural or biochemical abnormality [1,2]. IBS is categorized into subtypes according to the predominant bowel habit: diarrhea-predominant IBS, constipation -predominant IBS, and mixed pattern IBS [1]. In spite of the significant impact that IBS has on patient quality-of-life, currently available clinical treatments for IBS have proved unsatisfactory, mainly due to the difficulty in suppressing the visceral pain associated with IBS.

IBS is one of the most common gastrointestinal disorders, estimated to affect 7–15% of the general population in the USA and 6–12% in Asian countries [2,3]. Considering the health-care costs associated with treating the condition, the identification of effective therapies (such as the taking of supplements) that do not involve prescription drugs is beneficial [4,5].

Although the pathogenesis of IBS is not completely understood, studies have suggested that genetic factors, previous inflammation, mental stressors and microbiota play important roles [6]. A number of animal models for IBS has been established and used to evaluate clinical protocols designed to treat the condition. Mental stressor- or drug-induced alterations in defecation have been used as a model for defecation disorders related to IBS in animals [7–9]. Since hypersensitivity to colorectal distension (CRD) was observed in IBS patients [10], monitoring the electrical activity of the abdominal muscles (visceromotor response) in response to CRD is a standard procedure to detect IBS-related abdominal pain (visceral pain) in animals [11,12]. Furthermore, based on the increased colonic level of butyrate in IBS patients [13,14], butyrate enema-induced hypersensitivity to CRD is also considered as a useful animal model for IBS [15,16].

β-Glucans are naturally-occurring polysaccharides found in the cell walls of yeast, fungi, cereal plants and certain bacteria [17,18]. As suggested by the fact that various foods contain β-glucans, they are known to have few toxic and adverse effects [18]. β-Glucans from mushrooms have been used in Japan as anti-tumor drugs due to their immunostimulating activities [17]. In addition, β-(1,3)-D-glucans with β-(1,6) branches have been reported to have various clinically beneficial effects, such as enhancing the

Abbreviations: AUC, area under the curve; β-glucan, β-(1,3)-D-glucan with β-(1,6) branches; CRD, colorectal distention; 5-HT, 5-hydroxytryptamine hydrochlor ide; IBS, irritable bowel syndrome; LMW, low-molecular-weight; PBS, phosphate-buffered saline; S.E.M, standard error of the mean.

* Corresponding author at: Department of Analytical Chemistry, Faculty of Pharmacy, Keio University, 1-5-30 Shibakoen, Minato-ku, Tokyo 105-8512, Japan. Fax: +81 3 5400 2628.
E-mail address: mizushima-th@pha.keio.ac.jp (T. Mizushima).

0006-291X/$ - see front matter © 2012 Published by Elsevier Inc.
http://dx.doi.org/10.1016/j.bbrc.2012.03.015

bio-defense activity against bacterial, viral, fungal and parasitic challenge, increasing hematopoiesis and radioprotection, stimulating the wound healing response, and decreasing serum lipid levels [17–20]. Interestingly, it was recently reported that β-glucans suppress inflammatory responses in some animal models [21–26], suggesting that β-glucan could be an interesting immunomodulator, causing opposing effects on different aspects of the immune system.

We succeeded in the purification and industrial-scale production of low-molecular-weight β-(1,3–1,6)-D-glucan from *Aureobasidium pullulans* (*A. pullulans*) GM-NH-1A1 strain (LMW β-glucan) [27,28]. The characteristic features of LMW β-glucan are its low molecular weight (about 100 kDa), low viscosity, high water-solubility and high level of β-(1–6) branching (50–80%) [27,28]. We previously reported that LMW β-glucan has various clinically beneficial effects, such as suppression of the allergic response, suppression of restraint stress-induced immunosuppression and anti-tumor and anti-metastatic actions [27–29]. Moreover, we recently reported that LMW β-glucan protects the gastric mucosa against the formation of irritant-induced lesions by increasing levels of defensive factors such as heat shock protein 70 and gastric mucin [30]. In the present study, we use different animal models for IBS to test the hypothesis that LMW β-glucan could be effective in the treatment of this condition. Our results suggest that the oral administration of LMW β-glucan suppresses not only fecal pellet output but also the visceromotor response to CRD (visceral pain response). These findings suggest that LMW β-glucan could be therapeutically effective for the treatment of IBS.

2. Materials and methods

2.1. Chemicals and animals

LMW β-glucan was prepared from the conditioned culture medium of *A. pullulans* GM-NH-1A1, as described previously [27,28]. Analysis of ^{1}H and ^{13}C NMR spectra and gel-filtration chromatography revealed that the LMW β-glucan contains approximately 70% β-(1–6) branches and an average molecular weight of 100 kDa, as described previously [27,28]. Clonidine hydrochloride and castor oil were from WAKO Pure Chemicals (Osaka, Japan). Sodium butyrate, brewer's yeast and carbamyl- β-methylcholine chloride (bethanecol) were obtained from Sigma (St. Louis, MO). Loperamide hydrochloride and 5-hydroxytryptamine hydrochloride (5-HT) were purchased from Nacalai Tesque (Kyoto, Japan). Wild-type mice (C57/BL6, 6–8 weeks of age) and Wistar rats (4–6 weeks of age) were obtained from Charles River (Yokohama, Japan). Wistar-Imamichi rats (4 weeks of age) were purchased from the Institute for Animal Reproduction (Kasumigaura, Japan). The experiments and procedures described here were carried out in accordance with the Guide for the Care and Use of Laboratory Animals as adopted and promulgated by the National Institutes of Health, and were approved by the Animal Care Committees of Keio University and Kumamoto University.

2.2. Analysis of fecal pellet output in mice

Female mice were subjected to restraint stress by being placed individually into a 50 ml Falcon tube (Becton Dickinson, Franklin Lakes, NJ) for 1 h, as described previously [31]. These tubes are small enough to restrain a mouse so that it is able to breathe but unable to move freely. Control mice were left to move freely in the cage. The number of fecal pellets excreted during the 1-h restraint stress period was measured. β-Glucan was dissolved in phosphate-buffered saline (PBS) and administered orally 2 h before animals were subjected to the restraint stress. Control animals were administered PBS.

In a separate experiment, mice were administered one of different drugs that stimulate intestinal motility (bethanecol and 5-HT), cause diarrhea (castor oil) or cause constipation (loperamide and clonidine). Animals were then placed in a cage and the number or wet weight of fecal pellets excreted in the subsequent 1-, 2- or 24-h period determined. Drugs administered subcutaneously were bethanechol (3 mg/kg) and 5-HT (3 mg/kg), while those administered orally were loperamide (10 mg/kg), clonidine (3.5 mg/kg) and castor oil (300 μl/mouse).

β-Glucan was dissolved in PBS and administered orally 2 h before animals were subjected to the restraint stress or drug-treatment. Control animals were administered PBS.

2.3. Electromyography and CRD

Rats were deeply anaesthetized with pentobarbital sodium (40 mg/kg) and then electromyography electrodes (Star Medical, Tokyo, Japan) sutured into the external oblique muscle of the abdomen for electromyogram recording. Electrode leads were tunneled subcutaneously and exteriorized at the nape of the neck for future access. After surgery, rats were housed individually and allowed to recuperate for 6 days before being used for visceromotor response testing.

Repeated CRD was performed as described previously [32]. Rats were restrained in a plastic conical-shape tube (diameter, 6 cm; height, 15 cm), 15 min before electromyography. To reduce confounding effects due to restraint stress, rats were habituated to the tube 30 min per day for 3 days prior to the experiment. A polyethylene bag (length 2 cm) was inserted in the distal colon, positioned 1 cm proximal to rectum, and connected to a balloon catheter which was anchored with tape to the base of the tail. The pressure and volume of the balloon were controlled and monitored by a pressure controller-timing device (Distender Series II; G & J Electronics, Toronto, Canada), connected to the balloon. Rats were subjected to repeated CRD (80 mm Hg, 30 s, 5-min interstimulus interval, 12 times) on day 7. β-Glucan was given orally once daily for 7 days (from day 0 to day 6).

In separate experiments, CRD associated with the use of butyrate enemas was examined as described previously [15]. Rats were instilled with 1 ml sodium butyrate (110 mg/ml, pH 6.9) or saline into the colon twice daily for 3 days (day 1, 2 and 3). Rats were subjected to CRD (10, 20, 40 60 and 80 mm Hg, 20 s, 150-s interstimulus interval) on day 7. β-Glucan was given orally once daily for 7 days (from day 0 to day 6).

Visceromotor responses were monitored by electromyography, as described previously [11,33], 12 h after the last administration of β-glucan. Electromyograph data were collected and analyzed using 8 STAR software (version 6.0–19.2 for Windows; Star Medical, Tokyo, Japan). Responses evoked by contraction of the external oblique musculature were quantified by calculating the area under the curve (AUC) of the voltage alteration graph. The baseline was determined by data collected 20 s (butyrate enema) or 30 s (repeated CRD) before each distention.

2.4. Inflamed paw pressure nociception test

The pain threshold in Wistar-Imamichi rats was measured using a Randall–Sellito test with an analgometer (Ugo basile, Comerio, Italy), as described previously [34]. Brewer's yeast (20%, 1 ml) was injected into one of the hind paws. Seven hours later, an increasing pressure was applied to the underside of the hind limb and the pain threshold was defined as the pressure in grams eliciting a cry from the animal.

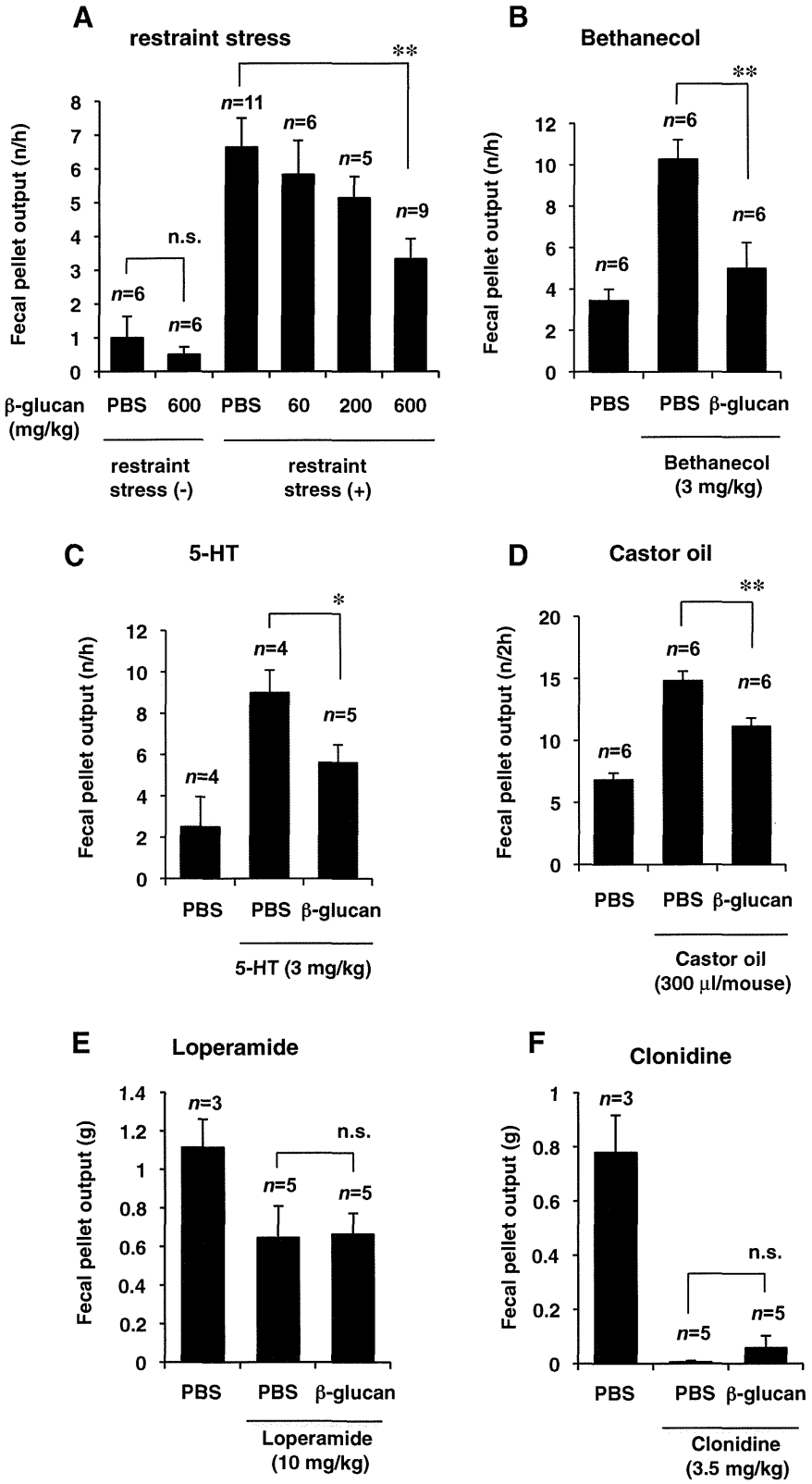

Fig. 1. Effects of LMW β-glucan on restraint stress- or drug-induced alteration of fecal pellet output in mice. Mice were orally administered indicated doses (A) or 600 mg/kg (B–F) of LMW β-glucan or vehicle (PBS). Two hours later, mice were exposed to restraint stress (A) or administered bethanecol (3 mg/kg, *s.c.*) (B), 5-HT (3 mg/kg, *s.c.*) (C), castor oil (300 μl/mouse, *p.o.*) (D), loperamide (10 mg/kg, *p.o.*) or clonidine (3.5 mg/kg, *p.o.*). The number (A–D) or wet weight (E and F) of fecal pellets excreted in the subsequent 0–1 h (A–C), 0–2 h (D) or 0–24 h (E and F) period was determined. Values are mean ± S.E.M $^{*}P < 0.05$; $^{**}P < 0.01$; n.s., not significant.

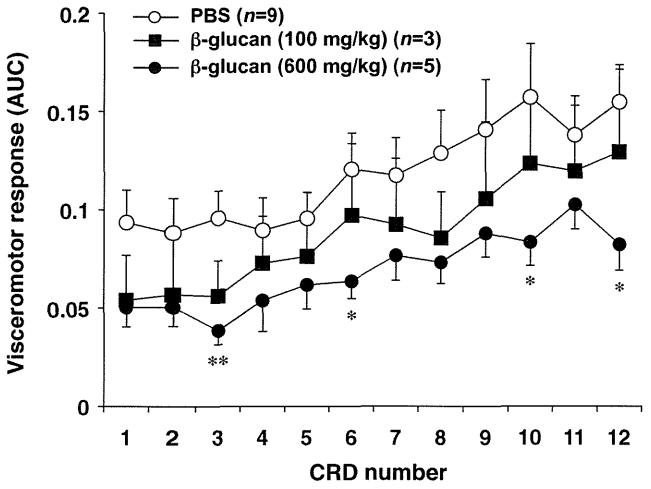

Fig. 2. Effect of LMW β-glucan on the viscermotor response to CRD in rats. The indicated doses (mg/kg) of β-glucan or PBS were orally administered to female Wistar rats once daily for 7 days. Twelve hours after the last administration of LMW β-glucan, rats were subjected to repetitive CRD and the visceromotor response was recorded and analysed as described in Section 2. Values are mean ± S.E.M $^{*}P < 0.05$; $^{**}P < 0.01$.

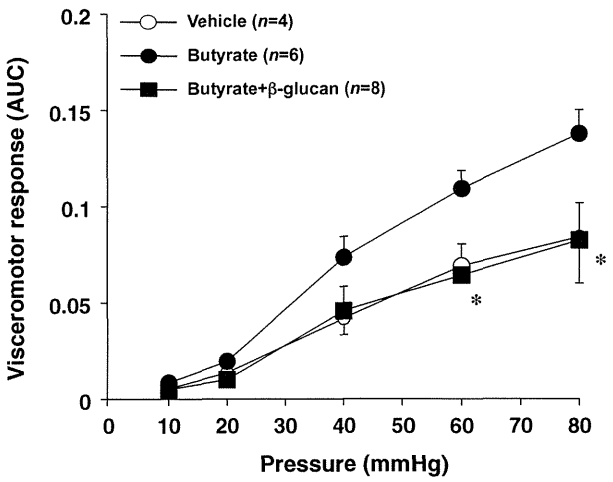

Fig. 3. Effect of LMW β-glucan on butyrate enema-induced colonic hypersensitivity to CRD in rats. Butyrate enemas were administered twice daily on days 1, 2 and 3. Administration of LMW β-glucan (600 mg/kg) (once daily from day 0 to day 6) and monitoring and analysis of the visceromotor response to CRD (on day 7) were performed as described in the legend of Fig. 2. Values are mean ± S.E.M $^{*}P < 0.05$.

2.5. Statistical analysis

All values are expressed as the mean ± S.E.M. Two-way ANOVA followed by the Tukey test or a Student's *t* test for unpaired results was used to evaluate differences between more than two groups or between two groups, respectively. Differences were considered to be significant for values of $P < 0.05$.

3. Results and discussion

3.1. Effect of LMW β-glucan on fecal pellet output in mice

We first examined the effect of a once-only oral administration of LMW β-glucan on restraint stress-induced fecal pellet output in mice. In untreated mice (administered PBS vehicle only), restraint stress (restricted movement by placement of mouse in a 50 ml plastic tube) caused a more than 5-fold increase in fecal pellet output per hour compared to unrestrained mice (Fig. 1A), as described previously [35]. The once-only oral pre-administration of LMW β-glucan suppressed this increase in a dose-dependent manner without affecting the basal level (without restraint stress) of fecal pellet output (Fig. 1A). Similar results were observed in response to a once-daily oral administration of LMW β-glucan for 7 days (data not shown). The LMW β-glucan-dependent suppression of restraint stress-induced fecal pellet output was also confirmed in rats (data not shown).

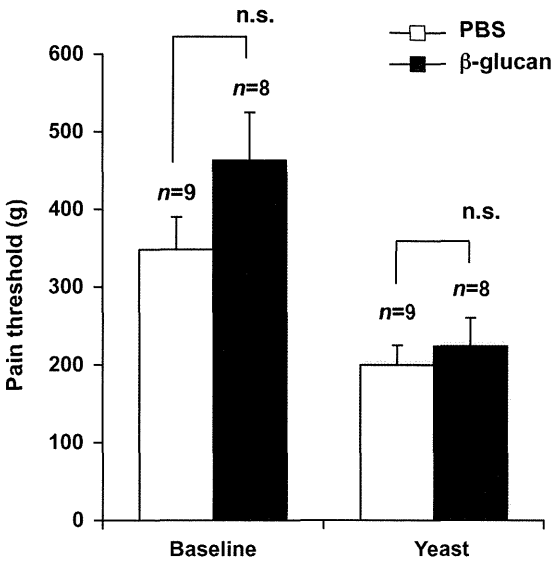

Fig. 4. Effect of LMW β-glucan on the pain response of rats in the inflamed paw pressure test. LMW β-glucan (600 mg/kg) was administered orally as described in the legend of Fig. 2. Twelve hours after the last administration of β-glucan, the inflamed paw pressure test was performed as described in Section 2. The pain threshold before (baseline) and after (yeast) the yeast injection was determined. Values are mean ± S.E.M n.s., not significant.

We also examined the effect of LMW β-glucan on the fecal pellet output induced by drugs that increase intestinal motility (bethanecol and 5-HT) or cause diarrhea (castor oil) [8,36]. As shown in Fig. 1B–D, the oral administration of LMW β-glucan (600 mg/kg) to mice suppressed the fecal pellet output induced by each of these drugs.

We then examined the effect of LMW β-glucan on drug-induced constipation. As shown in Fig. 1E and F, administration of loperamide or clonidine to mice decreased fecal pellet output, as described previously [36]. The oral pre-administration of LMW β-glucan did not alter the fecal pellet output. The results in Fig. 1 thus suggest that orally administered LMW β-glucan suppresses the restraint stress- or drug-induced stimulation of intestinal motility but does not affect the motility in the absence of these stimuli or in presence of constipation-inducing drugs. The mechanism underlying the LMW β-glucan-dependent suppression of intestinal motility is not clear at present.

3.2. Effect of LMW β-glucan on the visceromotor response to CRD in rats

In addition to alterations of fecal pellet output, hypersensitivity to visceral pain is one of the principle pathogenetic pathways for IBS. To study this phenomenon, we examined the effect of LMW β-glucan on visceromotor response to CRD, which has been used as an index of visceral pain response [33]. Rats were used for this analysis since the techniques for measuring the visceromotor response and CRD were established with these animals. As a single oral administration of LMW β-glucan did not significantly affect the visceromotor response to CRD (data not shown), we decided

to determine the effect of LMW β-glucan administered orally once-daily for 7 days. In control rats (PBS-treated), CRD evoked a visceromotor response which increased in amplitude in response to repeated CRDs (Fig. 2), as described previously [32]. Oral pre-administration of LMW β-glucan (600 mg/kg) to animals significantly decreased the visceromotor response to CRD not only after repetitive CRDs but also upon the first CRD (Fig. 2). Pre-administration of LMW β-glucan (100 mg/kg) also showed a tendency to decrease the visceromotor response to CRD, however the effect was not statistically significant (Fig. 2). These results indicate that oral pre-administration of high dose of LMW β-glucan suppresses the visceral pain response to CRD.

Since the visceromotor response to the first CRD was reduced by the pre-administration of LMW β-glucan, the results in Fig. 2 can be interpreted to indicate that LMW β-glucan suppresses the visceral pain response to CRD itself, but does not affect the repeated CRD-induced hypersensitivity to visceral pain. However, although we tried to habituate rats to the tube used for CRD experiment (see Section 2), it is possible that the animals entered into a state of restraint-like stress. Thus, it is also possible that LMW β-glucan suppresses the restraint stress-induced hypersensitivity to visceral pain.

We then examined the effect of LMW β-glucan on the visceral pain response in another animal model, butyrate-induced hypersensitivity to CRD. The butyrate enema is known to reduce the threshold of the visceromotor response to CRD [15,16]. We confirmed that twice-daily butyrate enemas (on days 1, 2 and 3) stimulated the visceromotor response to CRD on day 7 and found that when LMW β-glucan was orally pre-administered once daily from day 0 to day 6, the visceromotor response to CRD was similar to that measured in control rats (not given butyrate enemas) (Fig. 3). This result suggests that LMW β-glucan suppresses butyrate-induced hypersensitivity to CRD.

Finally, we tested whether the inhibitory effect of LMW β-glucan on the pain response is specific for visceral pain. For this purpose, we used the inflamed paw pressure test in which a yeast solution was administered to one of hind paws of rats to induce inflammation and the pressure-induced pain response was subsequently determined. As shown in Fig. 4, oral administration of LMW β-glucan once daily for 7 days did not affect the paw pressure required to elicit a nociception response (pain threshold) in both presence and absence of yeast injection. This finding suggests that LMW β-glucan does not affect the pain response in general but specifically affects the visceral pain response.

In conclusion, we have shown here that the oral administration of LMW β-glucan suppresses not only restraint stress- or drug-induced fecal pellet output, but also suppresses the visceral pain response. The difficulty associated with therapeutic management of IBS can be attributed to the fact that both abdominal pain and bowel habit disorders must be addressed. The results presented in this study thus suggest that LMW β-glucan could prove therapeutically beneficial for the prevention and treatment of IBS, especially in relation to the diarrhea-predominant IBS.

Acknowledgments

This work was supported by Grants-in-Aid of Scientific Research from the Ministry of Health, Labour, and Welfare of Japan, Grants-in-Aid for Scientific Research from the Ministry of Education, Culture, Sports, Science and Technology of Japan, and Grants-in-Aid of the Japan Science and Technology Agency.

References

[1] G.F. Longstreth, W.G. Thompson, W.D. Chey, L.A. Houghton, F. Mearin, R.C. Spiller, Functional bowel disorders, Gastroenterology 130 (2006) 1480–1491.
[2] D.A. Drossman, M. Camilleri, E.A. Mayer, W.E. Whitehead, AGA technical review on irritable bowel syndrome, Gastroenterology 123 (2002) 2108–2131.
[3] M. Shinozaki, S. Fukudo, M. Hongo, T. Shimosegawa, D. Sasaki, K. Matsueda, S. Harasawa, S. Miura, T. Mine, H. Kaneko, T. Arakawa, K. Haruma, A. Torii, T. Azuma, H. Miwa, M. Fukunaga, M. Handa, S. Kitamori, T. Miwa, High prevalence of irritable bowel syndrome in medical outpatients in Japan, J. Clin. Gastroenterol. 42 (2008) 1010–1016.
[4] C.W. Hammerle, C.M. Surawicz, Updates on treatment of irritable bowel syndrome, World J. Gastroenterol. 14 (2008) 2639–2649.
[5] D. Hulisz, The burden of illness of irritable bowel syndrome: current challenges and hope for the future, J Manag. Care Pharm. 10 (2004) 299–309.
[6] E.A. Mayer, S.M. Collins, Evolving pathophysiologic models of functional gastrointestinal disorders, Gastroenterology 122 (2002) 2032–2048.
[7] S. Okano, H. Nagaya, Y. Ikeura, H. Natsugari, N. Inatomi, Effects of TAK-637, a novel neurokinin-1 receptor antagonist, on colonic function in vivo, J. Pharmacol. Exp. Ther. 298 (2001) 559–564.
[8] S. Kobayashi, K. Ikeda, M. Suzuki, T. Yamada, K. Miyata, Effects of YM905, a novel muscarinic M3-receptor antagonist, on experimental models of bowel dysfunction in vivo, Jpn. J. Pharmacol. 86 (2001) 281–288.
[9] R. Moriya, T. Shirakura, H. Hirose, T. Kanno, J. Suzuki, A. Kanatani, NPY Y2 receptor agonist PYY(3–36) inhibits diarrhea by reducing intestinal fluid secretion and slowing colonic transit in mice, Peptides 31 (2010) 671–675.
[10] J. Munakata, B. Naliboff, F. Harraf, A. Kodner, T. Lembo, L. Chang, D.H. Silverman, E.A. Mayer, Repetitive sigmoid stimulation induces rectal hyperalgesia in patients with irritable bowel syndrome, Gastroenterology 112 (1997) 55–63.
[11] J.A. Christianson, G.F. Gebhart, Assessment of colon sensitivity by luminal distension in mice, Nat. Protoc. 2 (2007) 2624–2631.
[12] M. Larsson, S. Arvidsson, C. Ekman, A. Bayati, A model for chronic quantitative studies of colorectal sensitivity using balloon distension in conscious mice – effects of opioid receptor agonists, Neurogastroenterol. Motil. 15 (2003) 371–381.
[13] W.R. Treem, N. Ahsan, G. Kastoff, J.S. Hyams, Fecal short-chain fatty acids in patients with diarrhea-predominant irritable bowel syndrome: in vitro studies of carbohydrate fermentation, J. Pediatr. Gastroenterol. Nutr. 23 (1996) 280–286.
[14] C. Tana, Y. Umesaki, A. Imaoka, T. Handa, M. Kanazawa, S. Fukudo, Altered profiles of intestinal microbiota and organic acids may be the origin of symptoms in irritable bowel syndrome, Neurogastroenterol. Motil. 22 (2010) 512–519, e114–515.
[15] S. Bourdu, M. Dapoigny, E. Chapuy, F. Artigue, M.P. Vasson, P. Dechelotte, G. Bommelaer, A. Eschalier, D. Ardid, Rectal instillation of butyrate provides a novel clinically relevant model of noninflammatory colonic hypersensitivity in rats, Gastroenterology 128 (2005) 1996–2008.
[16] C. Rousseaux, X. Thuru, A. Gelot, N. Barnich, C. Neut, L. Dubuquoy, C. Dubuquoy, E. Merour, K. Geboes, M. Chamaillard, A. Ouwehand, G. Leyer, D. Carcano, J.F. Colombel, D. Ardid, P. Desreumaux, *Lactobacillus acidophilus* modulates intestinal pain and induces opioid and cannabinoid receptors, Nat. Med. 13 (2007) 35–37.
[17] J. Chen, R. Seviour, Medicinal importance of fungal beta-(1→3), (1→6)-glucans, Mycol. Res. 111 (2007) 635–652.
[18] S.V. Tsoni, G.D. Brown, Beta-Glucans and dectin-1, Ann. NY Acad. Sci. 1143 (2008) 45–60.
[19] M. Berdal, H.I. Appelbom, J.H. Eikrem, A. Lund, S. Zykova, L.T. Busund, R. Seljelid, T. Jenssen, Aminated beta-1,3-D-glucan improves wound healing in diabetic db/db mice, Wound Repair Regen. 15 (2007) 825–832.
[20] S. Bell, V.M. Goldman, B.R. Bistrian, A.H. Arnold, G. Ostroff, R.A. Forse, Effect of beta-glucan from oats and yeast on serum lipids, Crit. Rev. Food Sci. Nutr. 39 (1999) 189–202.
[21] G. Sener, E. Eksioglu-Demiralp, M. Cetiner, F. Ercan, B.C. Yegen, Beta-glucan ameliorates methotrexate-induced oxidative organ injury via its antioxidant and immunomodulatory effects, Eur. J. Pharmacol. 542 (2006) 170–178.
[22] A. Bedirli, M. Kerem, H. Pasaoglu, N. Akyurek, T. Tezcaner, S. Elbeg, L. Memis, O. Sakrak, Beta-glucan attenuates inflammatory cytokine release and prevents acute lung injury in an experimental model of sepsis, Shock 27 (2007) 397–401.
[23] O.I. Lyuksutova, E.D. Murphey, T.E. Toliver-Kinsky, C.Y. Lin, W. Cui, D.L. Williams, E.R. Sherwood, Glucan phosphate treatment attenuates burn-induced inflammation and improves resistance to *Pseudomonas aeruginosa* burn wound infection, Shock 23 (2005) 224–232.
[24] J. Soltys, M.T. Quinn, Modulation of endotoxin- and enterotoxin-induced cytokine release by in vivo treatment with beta-(1,6)-branched beta-(1,3)-glucan, Infect. Immun. 67 (1999) 244–252.
[25] H.Z. Toklu, A.O. Sehirli, A. Velioglu-Ogunc, S. Cetinel, G. Sener, Acetaminophen-induced toxicity is prevented by beta-D-glucan treatment in mice, Eur. J. Pharmacol. 543 (2006) 133–140.
[26] V.B. Shah, D.L. Williams, L. Keshvara, Beta-glucan attenuates TLR2- and TLR4-mediated cytokine production by microglia, Neurosci. Lett. 458 (2009) 111–115.
[27] Y. Kimura, M. Sumiyoshi, T. Suzuki, M. Sakanaka, Effects of water-soluble low-molecular-weight beta-1, 3-D-glucan (branch beta-1, 6) isolated from *Aureobasidium pullulans* 1A1 strain black yeast on restraint stress in mice, J. Pharm. Pharmacol. 59 (2007) 1137–1144.
[28] Y. Kimura, M. Sumiyoshi, T. Suzuki, M. Sakanaka, Antitumor and antimetastatic activity of a novel water-soluble low molecular weight beta-1, 3-D-glucan (branch beta-1,6) isolated from *Aureobasidium pullulans* 1A1 strain black yeast, Anticancer Res. 26 (2006) 4131–4141.

[29] Y. Kimura, M. Sumiyoshi, T. Suzuki, M. Sakanaka, Inhibitory effects of water-soluble low-molecular-weight beta-(1,3–1,6) D-glucan purified from *Aureobasidium pullulans* GM-NH-1A1 strain on food allergic reactions in mice, Int Immunopharmacol 7 (2007) 963–972.
[30] K. Tanaka, Y. Tanaka, T. Suzuki, T. Mizushima, Protective effect of beta-(1,3 → 1,6)-D-glucan against irritant-induced gastric lesions, Br. J. Nutr. 106 (2011) 475–485.
[31] T.L. Bale, R. Picetti, A. Contarino, G.F. Koob, W.W. Vale, K.F. Lee, Mice deficient for both corticotropin-releasing factor receptor 1 (CRFR1) and CRFR2 have an impaired stress response and display sexually dichotomous anxiety-like behavior, J. Neurosci. 22 (2002) 193–199.
[32] A. Ravnefjord, M. Brusberg, H. Larsson, E. Lindstrom, V. Martinez, Effects of pregabalin on visceral pain responses and colonic compliance in rats, Br. J. Pharmacol. 155 (2008) 407–416.
[33] K. Saito-Nakaya, R. Hasegawa, Y. Nagura, H. Ito, S. Fukudo, Corticotropin-releasing hormone receptor 1 antagonist blocks colonic hypersensitivity induced by a combination of inflammation and repetitive colorectal distension, Neurogastroenterol. Motil. 20 (2008) 1147–1156.
[34] L.O. Randall, J.J. Selitto, A method for measurement of analgesic activity on inflamed tissue, Arch. Int. Pharmacodyn. Ther. 111 (1957) 409–419.
[35] E. Mazzon, S. Cuzzocrea, Role of TNF-alpha in ileum tight junction alteration in mouse model of restraint stress, Am. J. Physiol. Gastrointest. Liver Physiol. 294 (2008) G1268–G1280.
[36] T. Saito, F. Mizutani, Y. Iwanaga, K. Morikawa, H. Kato, Laxative and anti-diarrheal activity of polycarbophil in mice and rats, Jpn. J. Pharmacol. 89 (2002) 133–141.

Review

Roles of oxidative stress in stomach disorders

Hidekazu Suzuki,[1,*] Toshihiro Nishizawa,[1,2] Hitoshi Tsugawa,[1] Sachiko Mogami[1] and Toshifumi Hibi[1]

[1]Division of Gastroenterology and Hepatology, Department of Internal Medicine, Keio University School of Medicine, 35 Shinanomachi, Shinjuku-ku, Tokyo 160-8582, Japan
[2]Division of Gastroenterology, National Hospital Organization Tokyo Medical Center, 2-5-1 Higashigaoka, Meguro-ku, Tokyo 152-8902, Japan

(Received 20 September, 2011; Accepted 29 September, 2011; Published online 9 December, 2011)

The stomach is a sensitive digestive organ that is susceptible and exposed to exogenous pathogens from the diet. In response to such pathogens, the stomach induces oxidative stress, which might be related to the development of gastric organic disorders such as gastritis, gastric ulcers, and gastric cancer, as well as functional disorders such as functional dyspepsia. In particular, the bacterium *Helicobacter pylori* plays a major role in eliciting and confronting oxidative stress in the stomach. The present paper summarizes the pathogenesis of oxidative stress in the stomach during the development of various stomach diseases.

Key Words*:** **gastric mucosa, oxidative stress, *Helicobacter pylori

Oxidative Stress in the Process of Gastric Mucosal Injury

Physiological responses to stressors include increased activity of the hypothalamic-pituitary-adrenal axis as well as changes in gastrointestinal tissue. According to Selye's formulation of the general adaptation syndrome, an increase in adrenocortical activity is related to an increase in the incidence of gastric ulceration. The main candidate for the cause of stress ulcers is oxidative stress. There is some evidence that psychological stress, in addition to physical stress such as surgical intervention and microbial infection including *Helicobacter pylori* (*H. pylori*),[1] leads to oxidative stress in the stomach. Oxidative stress, which is a state of elevated levels of reactive oxygen species (ROS), causes a variety of conditions that stimulate either additional ROS production or a decline in antioxidant defenses. Oxidative stress is not only involved in the pathogenesis of gastric inflammation, ulcerogenesis, and carcinogenesis in *H. pylori* infection, but also in that of lifestyle-related diseases including atherosclerosis, hypertension, diabetes mellitus, ischemic heart diseases, and malignancies.[2] Several phenotypes of gastrointestinal diseases, such as peptic ulcer disease and gastroparesis, are known to be related to antioxidant property dysfunction.

Ethanol. The effects of ethanol on gastric mucosa are complicated and multifaceted. They may be associated with a disturbance in the balance between gastric mucosal protective and aggressive factors. Gastric mucosa is exposed to gastric acid, pepsin, and stimulants among others, while gastroprotective factors maintain the integrity of the gastric mucous layer, microcirculatory system, HCO_3^-, prostaglandins (PGs), epidermal growth factor synthesis, and epithelial cell restitution. Ethanol injures the vascular endothelial cells of the gastric mucosa and induces microcirculatory disturbance and hypoxia, linking to the overproduction of oxygen radicals.

Pan *et al.*[3] report the role of mitochondrial energy charge in the pathogenesis of ethanol-induced gastric mucosal injury. The gastric mucosal lesion index is correlated with the thiobarbituric acid (TBA)-reactive substance (TBARS) content in gastric mucosa. As the concentration of ethanol increases and the exposure time to ethanol is extended, the TBARS content in gastric mucosa and the extent of gastric mucosal damage increase. The ultrastructural pathological changes in mitochondria are positively related to ethanol concentration and exposure time. The expressions of mitochondrial DNA ATPase subunits 6 and 8 mRNA decline with increasing TBARS content in gastric mucosa produced as a result of ethanol gavage. As mentioned above, ethanol-induced gastric mucosal injury is related to oxidative stress, which disturbs the energy metabolism of mitochondria and plays a critical role in the pathogenesis of ethanol-induced gastric mucosal injury.

Ischemia/reperfusion injury. Ischemia/reperfusion damages the gastric mucosa by inducing oxidative stress. Specifically, ROS such as superoxide (O_2^-) and hydrogen peroxide (H_2O_2) induce inflammatory responses and tissue damage by fragmenting cellular DNA. In the gut, ROS can also be generated by non-steroidal anti-inflammatory drugs (NSAIDs), cold stress, ethanol, and *H. pylori* infection. NADPH oxidase found in phagocytic cells, vascular smooth muscle cells, endothelial cells, fibroblasts, and adipocytes convert oxygen into superoxide anions. Nakagiri *et al.*[4] recently reported that NADPH oxidase activity is elevated in ischemia and ischemia/reperfusion and is involved in the resultant gastric mucosal damage. This increased NADPH oxidase activity may also upregulate cyclooxygenase-2.

Peskar *et al.*[5] report that during ischemia/reperfusion, inhibitors of the cyclooxygenase and lipoxygenase pathways increase gastric mucosal damage in a dose-dependent manner. The synergism observed as a result of the combination of cyclooxygenase and lipoxygenase inhibitors suggests that both pathways are important in gastric mucosal defense during ischemia/reperfusion. PGE_2 theoretically antagonizes the effects of cyclooxygenase and lipoxygenase inhibitors. Similarly, lipoxin A_4, a lipoxygenase-derived product of arachidonate metabolism, also antagonizes the effects of cyclooxygenase and lipoxygenase inhibitors; moreover, it could replace PGE_2 for the prevention of gastric mucosal damage caused by cyclooxygenase inhibitors during ischemia/reperfusion.

Portal hypertensive gastropathy. Portal hypertensive gastropathy (PHG) is a common complication of liver cirrhosis and is associated with impaired gastric mucosal healing. PHG may be related to increased ROS and lipid peroxide (LPO) production. Kinjo *et al.*[4] report increased levels of LPO and nitrotyrosine, an indicator of nitration of tyrosine residues due to peroxynitrite, in the gastric mucosa of portal hypertensive rats; in addition, they report impaired ERK1/2 phosphorylation related to increased nitration by peroxynitrite. The gastroprotective, anti-inflammatory agent rebamipide prevents free radical production by scavenging

*To whom correspondence should be addressed.
E-mail: hsuzuki@a6.keio.jp

He received "SFRR Japan Award of Scientific Excellent" in 2011 in recognition of his outstanding work.

doi: 10.3164/jcbn.11-115SR

hydroxyl radicals.[5,6] Rebamipide decreases LPO and nitrotyrosine levels, normalizes ERK1/2 phosphorylation, and improves the ulcer index; this suggests that defects in the mitogen-activated protein kinase (MAPK) pathway are involved in the increased susceptibility to gastric mucosal injury observed in portal hypertensive gastropathy, indicating a potential role of rebamipide for treatment.

NSAIDs and aspirin. In addition to inhibiting cyclooxygenase and decreasing prostaglandin production, NSAIDs induce mucosal damage *via* ROS produced by recruited leukocytes. ROS-mediated mitochondrial damage as well as lipid, protein, and DNA oxidation lead to apoptosis and mucosal injury. Proton pump inhibitor (PPI) therapy is thought to primarily protect gastric mucosa by inhibiting gastric acid secretion. Nevertheless, Maity *et al.*[7] recently demonstrated that a PPI, lansoprazole, also inhibits NSAID-induced gastropathy by inhibiting mitochondrial and Fas-mediated apoptosis pathways. Lansoprazole's anti-apoptotic activity appears to be mediated by preventing NSAID-induced reductions in anti-apoptotic genes (e.g., Bcl and Bcl-2) while inhibiting increases in Fas and Fas ligand as well as pro-apoptotic genes (e.g., Bax and Bak).

On the other hand, aspirin increases the permeability of cultured gastric epithelial cell monolayers. The disruption in barrier integrity is mediated by p38 MAPK and involves the downregulation of claudin-7, a protein component of tight junctions.[8] This differs from the effects of other NSAIDs (i.e., non-aspirin NSAIDs), which increase epithelial permeability coupled to cyclooxygenase-1 inhibition; this increase can be restored by PGE_2 administration.

Heat shock proteins. Heat shock proteins, especially HSP70, provide cellular protection against stressor-induced tissue damage by refolding or degrading denatured proteins produced as a result of these stressors. Otaka *et al.*[9] recently used affinity chromatography to identify cytoskeletal myosin and actin as the first molecules bound by HSP70 after gastric mucosal injury in rats. Transcriptional upregulation of HSPs occurs via the binding of the transcription factor, heat shock factor 1 (HSF1), to heat shock element, which is located upstream of the HSP genes. In HSF1 null and HSP70-expressing transgenic mice, HSPs protect against irritant (e.g., ethanol or NSAIDs)-induced gastric lesions; moreover, geranylgeranylacetone (GGA), a gastroprotective agent, induces HSPs. Furthermore, HSP70 protects the gastric mucosa by inhibiting apoptosis, proinflammatory cytokines, and cell adhesion molecules involved in leukocyte infiltration. After induction by GGA, HSPs exhibit protective effects in mouse models of inflammatory bowel disease as well as in NSAID-induced lesions of the small intestine. Therefore, HSP inducers such as GGA may have therapeutic benefits in numerous diseases.

Enlarged Fold Gastritis and Oxidative Stress

H. pylori eradication therapy increases Runt domain transcription factor 3 (RUNX3) expression in glandular epithelial cells in enlarged-fold gastritis. Recently, we reported that RUNX3 is expressed in gastric epithelial cells and that *H. pylori* eradication significantly increases RUNX3 expression in the glandular epithelium of the corpus; however, no changes were observed in the antrum.[10] The mucosal chemiluminescence value, a marker of oxidative stress, is 4-fold higher in the corpus than in the antrum. *H. pylori* eradication significantly decreases the mucosal chemiluminescence values in both portions of the stomach to nearly undetectable levels. We conclude that the glandular epithelium is exposed to high levels of carcinogenic oxidative stress and expresses low levels of the tumor-suppressing molecule, RUNX3; however, RUNX3 expression was restored after eradication, suggesting a high risk of carcinogenesis associated with *H. pylori*-induced enlarged-fold gastritis of the corpus.[10]

Oxidative Stress during *H. pylori* Infection

Antioxidant ability of *H. pylori* to establish chronic infection. *H. pylori* infection induces a strong inflammatory host response, leading to the generation of a number of ROS and reactive nitrogen species (RNS), which are mediated by neutrophils and macrophages.[11] The generation of ROS and/or RNS is an important host immune response against persistent pathogens. Therefore, *H. pylori* must combat oxidative stress generated by the host immune response using an antioxidant protein in order to establish long-term colonization.[12,13] The mechanisms for ROS detoxification are of particular interest in understanding the *H. pylori*-associated pathogenesis. It is well known that *H. pylori* has a variety of enzymes acting as antioxidant systems to combat the toxic effects of ROS including catalase (KatA), iron-cofactored superoxide dismutase (SodB), and alkyl hydroperoxide reductase (AhpC).[13,14]

Superoxide dismutase (SOD) catalyzes the conversion of superoxide anions to hydrogen peroxide, which is degraded to oxygen and water by catalase.[13,15] SOD is a metalloenzyme; 3 structurally different forms have been identified depending on the metal cofactor. In general, organisms encode different sets of SOD enzymes. For example, *Escherichia coli* has 3 SODs: Fe-SOD (SodB) and Mn-SOD (SodA) in the cytoplasm and Cu/Zn-SOD in the periplasm.[16] On the other hand, *H. pylori* produces only a single SodB encoded by the *sodB* gene.[17,18] It was recently reported that *sodB* deletion in *H. pylori* causes the bacterium to lose its capacity for gastric mucosal colonization in mice.[19] This indicates that SodB is an important determinant of the host colonization capability of *H. pylori*. The regulation of *sodB* mRNA expression is also important for ROS detoxification. The mRNA expression of *sodB* in *H. pylori* is directly regulated by ferric uptake regulator (Fur) protein.[20] Fur functions as a global transcriptional regulator in *H. pylori*.[21–24] It is reported that Fur binds to ferrous iron (Fe^{2+}) and that the genes for iron uptake are suppressed by the iron-binding form of Fur.[25,26] On the other hand, *sodB* expression is suppressed by the iron-free form of Fur (apo-Fur).[20] Apo-Fur binds to a specific consensus sequence called Fur-Box located on the *sodB* promoter, blocking the binding of RNA polymerase.[20,27,28] It was recently reported that nucleic-acid mutations in Fur-Box and/or amino-acid mutations in Fur decrease the affinity of apo-Fur for Fur-Box in *H. pylori*, halting the suppression of *sodB* mRNA expression.[29–31] In particular, stopping the suppression of *sodB* mRNA expression in *H. pylori* by amino-acid mutations in Fur (i.e., C78Y and P114S) determines the development of metronidazole (Mtz) resistance.[31] This is because, when Mtz enters cells, its antimicrobial toxicity is dependent on the reduction of its nitro group to nitro anion radicals and the generation of superoxide.[32,33]

The SodB of *H. pylori* shares 53% sequence identity with the corresponding protein from *E. coli*. Interestingly, *H. pylori* SodB is significantly different from other Fe-SODs; its most distinguishing characteristic is its extended C-terminal tail,[34] although the role of this tail remains unclear. The structure of SodB has been clarified; it is now known to exist as a dimer composed of 2 identical subunits.[34] Furthermore, it is identified as having 4 ferrous ion (Fe^{2+})-coordinating residues (i.e., an iron-binding domain; His 26, His 73, His 160, and Asp 156) (Fig. 1). In fact, SodB needs to recruit ferrous ion (Fe^{2+}) to express its activity.[15,34] It is expected that SodB activity might be suppressed by preventing the uptake of iron ion (Fe^{2+} and/or Fe^{3+}).

Generation of oxidative stress as a virulence factor in *H. pylori*-infected hosts. ROS released from activated neutrophils are also potential virulence factors involved in *H. pylori*-infected host cells. In *H. pylori*-infected host cells, hypochlorous anions (OCl^-) are generated from H_2O_2 in the presence of Cl^-. The hypochlorous anions subsequently react with ammonia (NH_3), which is derived from urea by urease produced by *H. pylori*,

doi: 10.3164/jcbn.11-115SR

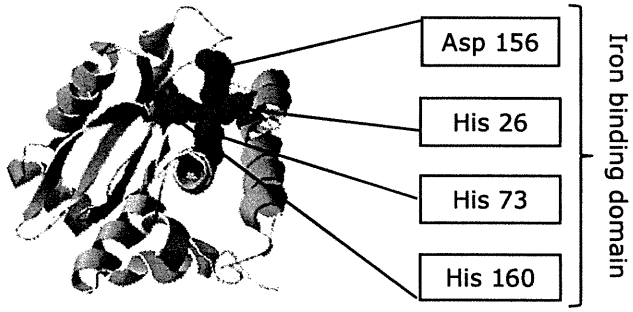

Fig. 1. Homology modeling of *Helicobacter pylori* SodB. Four amino acids (His 26, His 73, His 160, and Asp 156) of SodB are ferrous ion (Fe^{2+})-coordinating residues (i.e., an iron-binding domain).

ultimately yielding monochloramine (NH_2Cl). NH_2Cl induces mucosal cytotoxicity due to its lipophilic properties and freely penetrates biological membranes to oxidize intracellular components.[35–37]

In addition, it is well known that *H. pylori* produces a γ-glutamyltranspeptidase (EC 2.3.2.2; GGT) in the periplasm.[38] *H. pylori* GGT catalyzes the transpeptidation and hydrolysis of the γ-glutamyl groups of glutamine and glutathione. Interestingly, these findings indicate that *H. pylori* GGT performs 2 functions. First, GGT functions in the physiological functioning of *H. pylori*. *H. pylori* is unable to take up extracellular glutamine and glutathione directly; GGT hydrolyzes these substances to glutamate. The glutamate is then transported into *H. pylori* cells via a Na^+-dependent reaction and is mainly incorporated into the TCA cycle.[39] Second, GGT acts as a virulence factor by disrupting the antioxidant ability of host cells. Although glutathione has antioxidant potential in host cells, *H. pylori* GGT reduces extracellular glutathione levels. In fact, *H. pylori* GGT reduces the ROS resistance of the host cells and induces apoptosis or necrosis.[38,40]

Excess ROS are produced in *H. pylori*-colonized human stomachs; this induces oxidative stress to both the gastric mucosa and *H. pylori*. Because *H. pylori* has a deft capability of detoxifying ROS using a variety of enzymes to establish long-term colonization,[12,13] excess ROS leads solely to host cell damage.

Oxidative Stress in the Progression of Gastric Motility Disorders

Gastric motility disorders can occur in many clinical settings with a wide variety in the severity of symptoms with or without gastric mucosal injuries. Gastric motility disorders are attributable to either damage within the smooth muscle itself or dysfunctions within the neuromuscular components including the enteric nerves and interstitial cells of Cajal (ICC), which regulate smooth muscle function. How oxidative stress is involved in these dysfunctions is discussed in the following situations.

Gastrointestinal Complications in Sepsis

Oxygen radicals are implicated as relevant mediators in sepsis and septic shock in animals including humans.[41,42] Sepsis is a systemic response caused by bacterial endotoxins such as lipopolysaccharide, which induce the release of ROS and the generation of numerous pro-inflammatory factors and nitric oxide. During sepsis, the most frequent complications within the gastrointestinal tract are gastrointestinal motility disturbances and mucosal barrier dysfunction. Experimental administration of LPS delays gastric emptying and upregulates inducible nitric oxide synthase in order to downregulate neuronal nitric oxide synthase (nNOS) and synthesize PGs.[43] It is also reported that SOD reverses the endotoxin-induced delay in gastric emptying and diminishes the presence of nitrotyrosine, 4-hydroxy-2-nonenal in gastric mucosa, and inducible nitric oxide synthase-positive residential macrophages in the external musculature; these suggest the involvement of oxidative and nitrosative stresses in the pathogenesis of lipopolysaccharide-induced gastrointestinal dysmotility.[44]

Gastrointestinal Complications in Ischemia/Reperfusion Injury

The gastrointestinal tract is one of the most susceptible organ systems to ischemia. Previous investigations demonstrate that ischemia/reperfusion is a major contributor to gastric mucosal injury caused by stresses such as burn stress or hemorrhagic shock, NSAIDs, and *H. pylori* infection. In addition to mucosal injuries, delayed gastric emptying is also reported after gastric ischemia/reperfusion associated with disruption of the ICC network and nNOS-positive neurons.[45] ICC play critical roles in gastrointestinal motility in that they are the source of the electrical slow waves underlying the phasic contractions of the gastric musculature and mediate excitatory and inhibitory inputs to the musculature from the enteric motor neurons. Neuronal NOS generates neuronally derived NO, which is the major inhibitory neurotransmitter in the gastrointestinal tract. ICC and nNOS-positive neurons are both important factors for gastric emptying. Oxidative stress produced by the xanthine–xanthine oxidase system after ischemia/reperfusion may play a major role in these events, although the precise mechanism is unclear.

Diabetes Mellitus

Oxidative stress is a strong pathogenic co-factor involved in the development of complications of diabetes. Increased glucose levels in diabetes react non-enzymatically with proteins and become advanced glycation end products (AGEs); AGEs activate endothelial NADPH oxidase and increase endothelial ROS,[46] which occurs in animal models of diabetes[47] and diabetes patients.[48] Gastric neuromuscular dysfunction occurs in up to 30–50% of patients after 10 years of type 1 or 2 diabetes associated with histological changes including the loss of nNOS and ICC in both humans and animal models. It is reported that increased oxidative stress is attributable to the loss of upregulation of heme oxygenase-1; this results in the loss of ICC, decreased nNOS expression, and delayed gastric emptying in non-obese diabetic mice. These changes can be reversed by heme oxygenase-1 induction, demonstrating an important role of oxidative stress in the development of diabetic gastroparesis.[49]

Aging and Oxidative Stress

Gastrointestinal function declines with aging, including delayed gastric emptying, decreased peristalsis, and slowed colonic transit; these impair quality of life and increase morbidity and mortality. Notable changes in gut neuromuscular function that accompany advanced age are reported in human and animal models.[50,51] Cowen *et al.*[52] report a 50% reduction in ileal myenteric neurons in 24-month-old Sprague-Dawley rats fed *ad libitum*; this was prevented by caloric restriction, which reduces oxidative stress.[53] In the study using progeric mice deficient in the anti-aging peptide Klotho, progeric mice exhibited a gastric phenotype resembling that of human aging involving profound ICC loss with reduced slow wave amplitude and nitrergic inhibitory junction potentials. Klotho protects ICC by preserving their precursors, limiting oxidative stress, and maintaining nutritional status and normal levels of trophic factors important for ICC differentiation.[54] Increased oxidative stress in combination with a decrease

in circulating and tissue factors that regulate ICC differentiation and survival contribute to the profound depletion of mature ICC and impair gastric function.

Conclusion

In conclusion, oxidative stress is one of the major contributors to the development of stomach diseases. Recent therapeutic options such as gastroprotective agents including antioxidant properties (e.g., rebamipide) can modulate the level of oxidative stress to enhance anti-inflammatory or antioxidant capacity. The stomach is an organ in direct contact with external pathogens; by presenting a strong acid environment, it has a special biological defense mechanism that eliminates such pathogens. However, *H. pylori* manages to live in the stomach by breaking through this defensive line. In response to the colonization of this bacterium, gastric mucosa can be exposed to severe oxidative stress with considerable levels of inflammatory cell accumulation, which might be related to the development of gastric mucosal as well as neuromuscular disorders.

Acknowledgments

The present study was supported by a Grant-in-Aid for Scientific Research (B) from the Japan Society for the promotion of Science (No. 22300169, to H.S.), a grant of the Adaptable and Seamless Technology transfer Program through target-driven R&D (A-STEP) (AS231Z00132G to H.S.) from the Japan Science and Technology Agency (JST), a grant from the Smoking Research Foundation (to H.S.), the Keio Gijuku Academic Development Fund (to H.S.), and a Nateglinide Memorial Toyoshima Research and Education Fund (to H.S.).

Abbreviations

AGEs	advanced glycation end products
GGA	geranylgeranylacetone
GGT	γ-glutamyltranspeptidase
HSF	heat shock factor
ICC	interstitial cells of Cajal
LPO	lipid peroxide
MAPK	mitogen-activated protein kinase
Mtz	metronidazole
nNOS	neuronal nitric oxide synthase
NSAIDs	non-steroidal anti-inflammatory drugs
PGs	prostaglandins
PHG	portal hypertensive gastropathy
PPI	proton pump inhibitor
RNS	reactive nitrogen species
ROS	reactive oxygen species
RUNX3	Runt domain transcription factor 3
SOD	superoxide dismutase
TBARS	thiobarbituric acid-reactive substance

References

1 Suzuki H, Iwasaki E, Hibi T. *Helicobacter pylori* and gastric cancer. *Gastric Cancer* 2009; **12**: 79–87.
2 Suzuki H, Matsuzaki J, Hibi T. Ghrelin and oxidative stress in gastrointestinal tract. *J Clin Biochem Nutr* 2011; **48**: 122–125.
3 Pan JS, He SZ, Xu HZ, *et al.* Oxidative stress disturbs energy metabolism of mitochondria in ethanol-induced gastric mucosa injury. *World J Gastroenterol* 2008; **14**: 5857–5867.
4 Kinjo N, Kawanaka H, Akahoshi T, *et al.* Significance of ERK nitration in portal hypertensive gastropathy and its therapeutic implications. *Am J Physiol Gastrointest Liver Physiol* 2008; **295**: G1016–G1024.
5 Suzuki M, Miura S, Mori M, *et al.* Rebamipide, a novel antiulcer agent, attenuates *Helicobacter pylori* induced gastric mucosal cell injury associated with neutrophil derived oxidants. *Gut* 1994; **35**: 1375–1378.
6 Nishizawa T, Suzuki H, Nakagawa I, *et al.* Rebamipide-promoted restoration of gastric mucosal sonic hedgehog expression after early *Helicobacter pylori* eradication. *Digestion* 2009; **79**: 259–262.
7 Maity P, Bindu S, Choubey V, *et al.* Lansoprazole protects and heals gastric mucosa from non-steroidal anti-inflammatory drug (NSAID)-induced gastropathy by inhibiting mitochondrial as well as Fas-mediated death pathways with concurrent induction of mucosal cell renewal. *J Biol Chem* 2008; **283**: 14391–14401.
8 Oshima T, Miwa H, Joh T. Aspirin induces gastric epithelial barrier dysfunction by activating p38 MAPK via claudin-7. *Am J Physiol Cell Physiol* 2008; **295**: C800–C806.
9 Otaka M, Odashima M, Izumi Y, *et al.* Target molecules of molecular chaperone (HSP70 family) in injured gastric mucosa *in vivo*. *Life Sci* 2009; **84**: 664–667.
10 Suzuki M, Suzuki H, Minegishi Y, Ito K, Nishizawa T, Hibi T. *H. pylori*-eradication therapy increases RUNX3 expression in the glandular epithelial cells in enlarged-fold gastritis. *J Clin Biochem Nutr* 2010; **46**: 259–264.
11 Bagchi D, Bhattacharya G, Stohs SJ. Production of reactive oxygen species by gastric cells in association with *Helicobacter pylori*. *Free Radic Res* 1996; **24**: 439–450.
12 Allen LA. Phagocytosis and persistence of *Helicobacter pylori*. *Cell Microbiol* 2007; **9**: 817–828.
13 Wang G, Alamuri P, Maier RJ. The diverse antioxidant systems of *Helicobacter pylori*. *Mol Microbiol* 2006; **61**: 847–860.
14 Olczak AA, Olson JW, Maier RJ. Oxidative-stress resistance mutants of *Helicobacter pylori*. *J Bacteriol* 2002; **184**: 3186–3193.
15 Bereswill S, Neuner O, Strobel S, Kist M. Identification and molecular analysis of superoxide dismutase isoforms in *Helicobacter pylori*. *FEMS Microbiol Lett* 2000; **183**: 241–245.
16 Benov LT, Fridovich I. *Escherichia coli* expresses a copper- and zinc-containing superoxide dismutase. *J Biol Chem* 1994; **269**: 25310–25314.
17 Spiegelhalder C, Gerstenecker B, Kersten A, Schiltz E, Kist M. Purification of *Helicobacter pylori* superoxide dismutase and cloning and sequencing of the gene. *Infect Immun* 1993; **61**: 5315–5325.
18 Pesci EC, Pickett CL. Genetic organization and enzymatic activity of a superoxide dismutase from the microaerophilic human pathogen, *Helicobacter pylori*. *Gene* 1994; **143**: 111–116.
19 Seyler RW Jr., Olson JW, Maier RJ. Superoxide dismutase-deficient mutants of *Helicobacter pylori* are hypersensitive to oxidative stress and defective in host colonization. *Infect Immun* 2001; **69**: 4034–4040.
20 Ernst FD, Homuth G, Stoof J, *et al.* Iron-responsive regulation of the *Helicobacter pylori* iron-cofactored superoxide dismutase SodB is mediated by Fur. *J Bacteriol* 2005; **187**: 3687–3692.
21 Ernst FD, Bereswill S, Waidner B, *et al.* Transcriptional profiling of *Helicobacter pylori* Fur- and iron-regulated gene expression. *Microbiology* 2005; **151**: 533–546.
22 Lee HW, Choe YH, Kim DK, Jung SY, Lee NG. Proteomic analysis of a ferric uptake regulator mutant of *Helicobacter pylori*: regulation of *Helicobacter pylori* gene expression by ferric uptake regulator and iron. *Proteomics* 2004; **4**: 2014–2027.
23 Bijlsma JJ, Waidner B, Vliet AH, *et al.* The *Helicobacter pylori* homologue of the ferric uptake regulator is involved in acid resistance. *Infect Immun* 2002; **70**: 606–611.
24 Choi YW, Park SA, Lee HW, Lee NG. Alteration of growth-phase-dependent protein regulation by a Fur mutation in *Helicobacter pylori*. *FEMS Microbiol Lett* 2009; **294**: 102–110.
25 Delany I, Pacheco AB, Spohn G, Rappuoli R, Scarlato V. Iron-dependent transcription of the frpB gene of *Helicobacter pylori* is controlled by the Fur repressor protein. *J Bacteriol* 2001; **183**: 4932–4937.
26 van Vliet AH, Stoof J, Vlasblom R, *et al.* The role of the ferric uptake regulator (Fur) in regulation of *Helicobacter pylori* iron uptake. *Helicobacter* 2002; **7**: 237–244.
27 Tiss A, Barre O, Michaud-Soret I, Forest E. Characterization of the DNA-binding site in the ferric uptake regulator protein from *Escherichia coli* by UV crosslinking and mass spectrometry. *FEBS Lett* 2005; **579**: 5454–5460.

doi: 10.3164/jcbn.11-115SR

28 Baichoo N, Helmann JD. Recognition of DNA by Fur: a reinterpretation of the Fur box consensus sequence. *J Bacteriol* 2002; **184**: 5826–5832.
29 Carpenter BM, Gancz H, Gonzalez-Nieves RP, *et al.* A single nucleotide change affects fur-dependent regulation of sodB in *H. pylori*. *PLoS One* 2009; **4**: e5369.
30 Choi SS, Chivers PT, Berg DE. Point mutations in *Helicobacter pylori*'s fur regulatory gene that alter resistance to metronidazole, a prodrug activated by chemical reduction. *PLoS One* 2011; **6**: e18236.
31 Tsugawa H, Suzuki H, Satoh K, *et al.* Two amino acids mutation of ferric uptake regulator determines *Helicobacter pylori* resistance to metronidazole. *Antioxid Redox Signal* 2011; **14**: 15–23.
32 Perez-Reyes E, Kalyanaraman B, Mason RP. The reductive metabolism of metronidazole and ronidazole by aerobic liver microsomes. *Mol Pharmacol* 1980; **17**: 239–244.
33 Rao DN, Mason RP. Generation of nitro radical anions of some 5-nitrofurans, 2- and 5-nitroimidazoles by norepinephrine, dopamine, and serotonin. A possible mechanism for neurotoxicity caused by nitroheterocyclic drugs. *J Biol Chem* 1987; **262**: 11731–11736.
34 Esposito L, Seydel A, Aiello R, *et al.* The crystal structure of the superoxide dismutase from *Helicobacter pylori* reveals a structured C-terminal extension. *Biochim Biophys Acta* 2008; **1784**: 1601–1606.
35 Suzuki M, Miura S, Suematsu M, *et al. Helicobacter pylori*-associated ammonia production enhances neutrophil-dependent gastric mucosal cell injury. *Am J Physiol* 1992; **263**: G719–G725.
36 Suzuki H, Mori M, Suzuki M, Sakurai K, Miura S, Ishii H. Extensive DNA damage induced by monochloramine in gastric cells. *Cancer Lett* 1997; **115**: 243–248.
37 Suzuki H, Seto K, Mori M, Suzuki M, Miura S, Ishii H. Monochloramine induced DNA fragmentation in gastric cell line MKN45. *Am J Physiol* 1998; **275**: G712–G716.
38 Shibayama K, Kamachi K, Nagata N, *et al.* A novel apoptosis-inducing protein from *Helicobacter pylori*. *Mol Microbiol* 2003; **47**: 443–451.
39 Shibayama K, Wachino J, Arakawa Y, Saidijam M, Rutherford NG, Henderson PJ. Metabolism of glutamine and glutathione via gamma-glutamyltranspeptidase and glutamate transport in *Helicobacter pylori*: possible significance in the pathophysiology of the organism. *Mol Microbiol* 2007; **64**: 396–406.
40 Flahou B, Haesebrouck F, Chiers K, *et al.* Gastric epithelial cell death caused by *Helicobacter suis* and *Helicobacter pylori* γ-glutamyl transpeptidase is mainly glutathione degradation-dependent. *Cell Microbiol* 2011; **13**: 1933–1955.
41 Goode HF, Webster NR. Free radicals and antioxidants in sepsis. *Crit Care Med* 1993; **21**: 1770–1776.
42 Albuszies G, Brückner UB. Antioxidant therapy in sepsis. *Intensive Care Med* 2003; **29**: 1632–1636.
43 Calatayud S, García-Zaragozá E, Hernández C, *et al.* Downregulation of nNOS and synthesis of PGs associated with endotoxin-induced delay in gastric emptying. *Am J Physiol Gastrointest Liver Physiol* 2002; **283**: G1360–G1367.
44 de Winter BY, van Nassauw L, de Man JG. Role of oxidative stress in the pathogenesis of septic ileus in mice. *Neurogastroenterol Motil* 2005; **17**: 251–261.
45 Suzuki S, Suzuki H, Horiguchi K, *et al.* Delayed gastric emptying and disruption of the interstitial cells of Cajal network after gastric ischaemia and reperfusion. *Neurogastroenterol Motil* 2010; **22**: 585–593, e126.
46 Wautier MP, Chappey O, Corda S, Stern DM, Schmidt AM, Wautier JL. Activation of NADPH oxidase by AGE links oxidant stress to altered gene expression via RAGE. *Am J Physiol Endocrinol Metab* 2001; **280**: E685–E694.
47 Hink U, Li H, Mollnau H, Oelze M, *et al.* Mechanisms underlying endothelial dysfunction in diabetes mellitus. *Circ Res* 2001; **88**: E14–E22.
48 Guzik TJ, West NE, Black E, *et al.* Vascular superoxide production by NAD(P)H oxidase: association with endothelial dysfunction and clinical risk factors. *Circ Res* 2000; **86**: E85–E90.
49 Choi KM, Gibbons SJ, Nguyen TV, *et al.* Heme oxygenase-1 protects interstitial cells of Cajal from oxidative stress and reverses diabetic gastroparesis. *Gastroenterology* 2008; **135**: 2055–2064, 2064 e1-2.
50 Horowitz M, Maddern GJ, Chatterton BE, Collins PJ, Harding PE, Shearman DJ. Changes in gastric emptying rates with age. *Clin Sci (Lond)* 1984; **67**: 213–218.
51 Phillips RJ, Powley TL. As the gut ages: timetables for aging of innervation vary by organ in the Fischer 344 rat. *J Comp Neurol* 2001; **434**: 358–377.
52 Cowen T, Johnson RJ, Soubeyre V, Santer RM. Restricted diet rescues rat enteric motor neurons from age related cell death. *Gut* 2000; **47**: 653–660.
53 Qiu X, Brown K, Hirschey MD, Verdin E, Chen D. Calorie restriction reduces oxidative stress by SIRT3-mediated SOD2 activation. *Cell Metab* 2010; **12**: 662–667.
54 Izbeki F, Asuzu DT, Lorincz A, *et al.* Loss of Kitlow progenitors, reduced stem cell factor and high oxidative stress underlie gastric dysfunction in progeric mice. *J Physiol* 2010; **588**: 3101–3117.

Dig Dis Sci (2012) 57:858–864
DOI 10.1007/s10620-011-1953-y

ORIGINAL ARTICLE

Enhanced Gastric Ghrelin Production and Secretion in Rats with Gastric Outlet Obstruction

Eisuke Iwasaki · Hidekazu Suzuki · Tatsuhiro Masaoka · Toshihiro Nishizawa · Hiroshi Hosoda · Kenji Kangawa · Toshifumi Hibi

Received: 7 September 2011 / Accepted: 12 October 2011 / Published online: 4 November 2011

Abstract
Background and Aim Ghrelin has distinct effects on gastrointestinal motility through the vagus nerve and gastric excitatory neural plexus. The objectives of this study were to investigate the dynamics of ghrelin and expression of neuromuscular markers in a newly established surgically manipulated rat model of gastric outlet obstruction (GOO), akin to the pyloric stricture associated with duodenal ulcer, advanced gastric cancer, and other conditions, in the clinical setting.
Material and Methods The rats were divided into two groups, a control group (sham operation) and the GOO group (proximal duodenal stricture). The animals were sacrificed 2 weeks after the operation. Plasma and gastric ghrelin were measured by radioimmunoassay. mRNA expression in the stomach of neural choline acetyltransferase (ChAT), c-kit, and membrane-bound stem cell factor (SCF) were analyzed by quantitative RT-PCR. In addition, gastric mRNA expression of the aforementioned were also evaluated 60 min after intraperitoneal administration of a synthetic GHS-R1a antagonist ([D-Lys3] GHRP-6 6.0 mg/kg).
Results Mechanical GOO induced increases of fasting plasma ghrelin levels and hyperplasia of the gastric muscle layers, with enhanced expression of the gastric neuromuscular markers. Administration of [D-Lys3] GHRP-6 normalized the enhanced expression of c-kit and SCF.
Conclusion GOO stimulates ghrelin dynamics and then enhances the mechanistic expression of gastric cellular communication network molecules between nerves and smooth muscle cells.

Keywords Ghrelin · Gastric emptying · Motility · Gastric outlet obstruction

Introduction

Ghrelin, a 28-amino-acid motilin-related peptide, was first purified from the rat stomach as a natural ligand for the growth hormone secretagogue receptor (GHSR) [1]. It has also been shown to stimulate food intake, induce body weight gain, and enhance gastric motility. Recent animal studies have shown that ghrelin has distinct effects on gastrointestinal motility, which may be mediated through the GHSR expressed on the vagus nerve and enteric nerve endings [2, 3]. Ghrelin has been reported to enhance gastric motility and accelerate gastric emptying in rats and mice and to stimulate small intestinal transit [2, 4]. Fujino et al. reported that ghrelin induces accelerated motor activity of the gastrointestinal tract via ghrelin receptors expressed on vagal afferent nerve terminals and activated neuropeptide Y neurons in the brain [5].

Chasen et al. reported that abnormal electrogastrography diagnosis and increased levels of plasma ghrelin were

E. Iwasaki · H. Suzuki (✉) · T. Masaoka · T. Nishizawa · T. Hibi
Division of Gastroenterology and Hepatology, Department of Internal Medicine, Keio University School of Medicine, 35 Shinanomachi, Shinjuku-ku, Tokyo 160-8582, Japan
e-mail: hsuzuki@a6.keio.jp

E. Iwasaki
Department of Internal Medicine, Saiseikai Central Hospital, 1-4-17 Mita, Minato-ku, Tokyo 108-0073, Japan

H. Hosoda · K. Kangawa
Department of Biochemistry, National Cardiovascular Center Research Institute, 5-7-1 Fujishiro-dai, Suita, Osaka 565-8565, Japan

found in most patients with advanced cancer [6]. We have previously shown increased fasting plasma levels of ghrelin in patients with functional dyspepsia (FD), especially those with dysmotility-like FD, possibly originating from gastric motility disorders, including delayed gastric emptying [7]. Although the precise molecular mechanisms are not yet clear, such clinical manifestations suggest that ghrelin production might be increased by impaired gastric motility.

The objectives of this study were to investigate the dynamics of ghrelin and expression of neuromuscular markers in a newly established surgically manipulated rat model of gastric outlet obstruction (GOO), akin to the pyloric stricture associated with duodenal ulcer, advanced gastric cancer, and other clinical conditions.

Methods

Animal Procedures

This study was conducted with the approval of Keio University Animal Research Committee (no. 056188). Seven-week-old male specific-pathogen-free (SPF) Sprague–Dawley (SD) rats (Sankyo Laboratory Service, Tokyo, Japan) were used for the study after acclimatization for 7 days in an animal room at a controlled temperature (24 ± 2°C). The rats were fed standard chow and deprived of food for 24 h before the operation. After induction of anesthesia by intraperitoneal injection of 50 mg/kg sodium pentobarbital, the hair was shaved off the upper abdomen of the animals. The abdomen was opened via a 25-mm-long median incision, and the stomach was exposed. The proximal duodenum was then carefully covered with an 18-Fr Nelaton catheter (diameter, 4.0 mm; Nippon Sherwood, Tokyo, Japan) and sutured with a 5–0 nylon thread (Fig. 1). The width of the catheter was 2.0 mm. This surgical duodenal stricture induced incomplete gastric outlet obstruction with gastric retention; this animal group was named the GOO group. After the operation, the animals were deprived of food for 24 h, but allowed free access to water. A sham operation, involving only abdominal incision, was also undertaken on the same number of rats of the control group.

Because weight loss is known to increase circulating levels of ghrelin, we designed a pair-feeding method to evaluate the dynamics of ghrelin without the confounding effect of body weight changes. The results of our preliminary experiments revealed that food intake in the GOO group was lower than that in the control group. We measured daily food intake in the GOO group, and the control group of rats received the same amount of food on the following day. After 2 weeks, after food deprivation for 24 h, the rats were sacrificed under ether anesthesia and the gastric wet weight and intraluminal pH were measured. The thicknesses of the gastric antral mucosal layer and muscular layer were measured by light-microscopic examination of hematoxylin–eosin-stained sections. The average thicknesses 1, 1.5, and 2.0 mm from the pylorus were measured.

Evaluation of Gastric Emptying

Our surgical procedure is the first reported method for establishing an animal model of GOO. We compared the gastric emptying rate in this model with that in another group of 7-week-old SPF male SD rats. The animals were divided into a control group and GOO group as previously described. Two weeks after the operation, the rats were deprived of food, but allowed free access to water for 24 h before the start of the subsequent experiment. The gastric emptying rate was measured by the phenol red (PR) method reported by Ohnishi et al. [8]. One milliliter of PR (100 μg/ml) was administered orally to the rats, and the rats were sacrificed by cervical dislocation either immediately (Control group, $n = 4$) or 15 min (Control group, $n = 4$; GOO group, $n = 6$) after administration of the PR solution. The standard stomachs (0 min) and test stomachs (15 min) were exposed and ligated at the cardia and pylorus. Each stomach was removed and placed in 10 ml 0.1 M Na_2HPO_4 solution, and the contents of the stomach were washed out. The absorbance of the supernatant was measured at 570 nm with a spectrometer (Shimadzu, Kyoto, Japan). The gastric emptying rate for each rat was calculated as described previously [8].

Measurement of the Ghrelin Dynamics

The rats were divided into two groups, the control group ($n = 14$) and the GOO group ($n = 14$). After 2 weeks, following food deprivation for 24 h, the rats were sacrificed under ether anesthesia. The abdomen and chest were opened via a median incision. Blood was collected from the heart and centrifuged at 3,000 rpm for 10 min to obtain plasma and serum samples for assay. After collection of the blood, the stomachs of the animals were excised and the intraluminal pH was examined by use of a pH meter (Horiba Techno Service, Kyoto, Japan). The stomachs were then cut along the greater curvature and rinsed with isotonic saline. The two radioimmunoassays (RIAs) for measurement of the gastric and plasma ghrelin levels were performed as described previously [9, 10]. Two polyclonal rabbit antibodies were raised against the N-terminal [1–11] (Gly1-Lys11) and C-terminal [13–28] (Gln13-Arg28) fragments of rat ghrelin. [Cys12]-rat ghrelin [1–11] (4 mg) and [Cys0]-rat ghrelin [13–28] (10 mg) were separately conjugated to maleimide-activated mariculture keyhole limpet hemocyanin (mcKLH, Pierce, Rockford, IL, USA; 6 mg) in conjugation buffer (Pierce). Each conjugate was

emulsified with an equal volume of Freund's complete adjuvant. Two corresponding batches of antiserum were obtained by immunization of New Zealand white rabbits by subcutaneous injection. Using these antibodies, two types of RIAs to measure the plasma and gastric ghrelin levels were performed as described previously [11].

Immunohistochemistry for Ghrelin

Stomach samples were fixed in 10% formaldehyde neutral buffer solution for 24 h, then embedded in paraffin. Tissue sections were deparaffinized and hydrated, and endogenous peroxidase was quenched by treatment with 0.3% hydrogen peroxide for 20 min. Nonspecific binding was blocked by use of a blocking reagent (BlockAce; Dainippon Pharmaceuticals, Osaka, Japan). After washing with TBS-T, the tissue slices were incubated for 60 min at 4°C with anti-ghrelin antiserum (final dilution, 1:10,000). Then, after washing again with TBS-T, the slides were incubated with EnVision + Peroxidase rabbit (DAKO Japan, Kyoto, Japan) for 30 min at room temperature, and then visualized after color development with 3,3′-diaminobenzidine tetrahydrochloride (DAB) solution for 1 min. The sections were then counterstained with hematoxylin. The stained sections were examined under high-power magnification (objective lens ×40) by light microscopy equipped with a 3CCD digital camera (C7780; Hamamatsu Photonics, Hamamatsu, Japan). The nuclei were counted using Image-J software (National Institutes of Health, Bethesda, Maryland, USA). The density of the ghrelin-immunoreactive cells was computed by use of the equation: Dghrelin = (Ng/Nt) × 100 (%), where Ng and Nt represent the number of ghrelin-immunoreactive cells and the total cell number, respectively, in the three mucosal regions of the stomach.

Preparation of Total RNA and Quantitative RT-PCR Analysis

Total mRNA was extracted from the stomach tissue by use of the RNeasy Mini Kit (Qiagen, Valencia, CA, USA), and DNase treatment was performed with an RNase-free DNase set (Qiagen). RNA was converted into cDNA by use of the PrimeScript RT reagent kit (Takara, Ohtsu, Japan). Cyber green quantitative real-time RT-PCR was performed to detect the mRNA using the Thermal Cycler Dice Real Time System (Takara Bio, Otsu, Japan). The primers used to amplify the target mRNA were: c-kit mRNA 5′-ATC CAG CCC CAC ACC CTG TT-3′, and 5′-TGT AGG CAA GAA CCA TCA CAA TGA-3′, SCF (membrane-bound isoform) mRNA: 5′-TGA GAA AGG GAA AGC CGC-3′, and 5′-TAA GGC TCC AAA AGC AAA GC-3′, choline acetyltransferase (ChAT) mRNA: 5′-CAA CCA TCT TCT GGC ACT GA-3′, and 5′-TAG CAG GCT CCA TAG CCA TT-3′, glyceraldehyde-3-phosphate (GAPDH) mRNA: 5′-GGC ACA GTC AAG GCT GAG AAT G-3′, and 5′-ATG GTG GTG AAG ACG CCA GTA-3′. The target mRNA expression levels were normalized to the GAPDH mRNA expression levels.

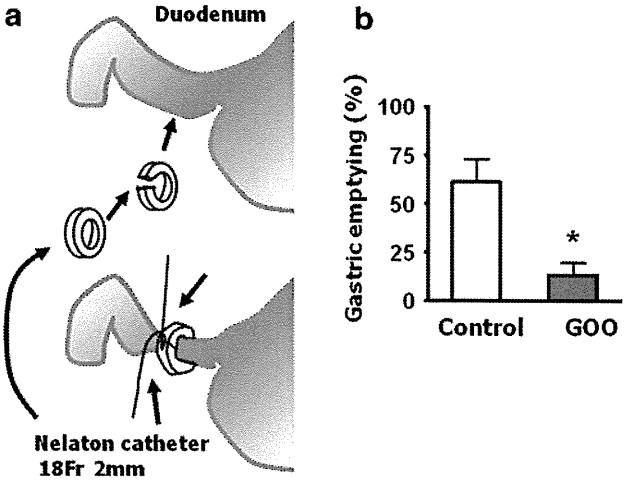

Fig. 1 **a** Surgical manipulation for induction of duodenal stricture. The proximal duodenum was covered with a small piece of an 18Fr-Nelaton catheter. **b** Liquid gastric emptying rates of control rats ($n = 4$, *open bar*) and GOO rats ($n = 6$, *filled bar*) 2 weeks after the operation (mean ± S.E.M. $^*P < 0.05$ compared with control)

RT-PCR Analysis for Interstitial Cells of the Cajal (ICC) Network Using a GHSR1a Antagonist

In a separate experiment, to examine the relationship between ghrelin and neuromuscular marker expression, the rats were administered an intraperitoneal injection of [D-Lys3] GHRP-6, a GHSR antagonist, (6.0 mg/kg; Bachem, King of Prussia, PA, USA) in 1 ml saline ($n = 8$), or saline alone ($n = 8$) and then euthanized 60 min after administration. Then, the mRNA expression levels of c-kit, SCF, and ChAT were analyzed by quantitative RT-PCR, as previously described.

Statistical Analysis

All results are expressed as mean ± SE, and the statistical analysis was performed using the Student t test (two-tailed test) with Stat Mate III (Atoms, Tokyo, Japan). P values less than 0.05 were considered to be statistically significant.

Results

Gastric Emptying Rate in this Rat Model

The gastric emptying rate after 15 min as measured by the PR method was significantly lower in the GOO group than